

7. Shiota M, Fujimoto J, Semba T, Satoh H, Yamamoto T, Mori S: Hyperphosphorylation of a novel 80 kDa protein-tyrosine kinase similar to Ltk in a human Ki-1 lymphoma cell line, AMS3. *Oncogene* 1994, 9:1567-1574
8. Bridge JA, Kanamori M, Ma Z, Pickering D, Hill DA, Lydiatt W, Lui MY, Colleoni GW, Antonescu CR, Ladanyi M, Morris SW: Fusion of the ALK gene to the clathrin heavy chain gene, CLTC, in inflammatory myofibroblastic tumor. *Am J Pathol* 2001, 159:411-415
9. Iwahara T, Fujimoto J, Wen D, Cupples R, Bucay N, Arakawa T, Mori S, Ratzkin B, Yamamoto T: Molecular characterization of ALK, a receptor tyrosine kinase expressed specifically in the nervous system. *Oncogene* 1997, 14:439-449
10. Morris SW, Naeve C, Mathew P, James PL, Kirstein MN, Cui X, Witte DP: ALK, the chromosome 2 gene locus altered by the t(2;5) in non-Hodgkin's lymphoma, encodes a novel neural receptor tyrosine kinase that is highly related to leukocyte tyrosine kinase (LTK). *Oncogene* 1997, 14:2175-2188
11. Ben-Neriah Y, Bauskin AR: Leukocytes express a novel gene encoding a putative transmembrane protein-kinase devoid of an extracellular domain. *Nature* 1988, 333:672-676
12. Maru Y, Hirai H, Takaku F: Human Itk: gene structure and preferential expression in human leukemic cells. *Oncogene Res* 1990, 5:199-204
13. Bernardis A, de la Monte SM: The Itk receptor tyrosine kinase is expressed in pre-B lymphocytes and cerebral neurons and uses a non-AUG translational initiator. *EMBO J* 1990, 9:2279-2287
14. Pulford K, Lamant L, Morris SW, Butler LH, Wood KM, Stroud D, Delsol G, Mason DY: Detection of anaplastic lymphoma kinase (ALK) and nucleolar protein nucleophosmin (NPM)-ALK proteins in normal and neoplastic cells with the monoclonal antibody ALK1. *Blood* 1997, 89:1394-1404
15. Shiota M, Fujimoto J, Takenaga M, Satoh H, Ichinohasama R, Abe M, Nakano M, Yamamoto T, Mori S: Diagnosis of t(2;5)(p23;q35)-associated Ki-1 lymphoma with immunohistochemistry. *Blood* 1994, 84:3648-3652
16. Duyster J, Bai RY, Morris SW: Translocations involving anaplastic lymphoma kinase (ALK). *Oncogene* 2001, 20:5623-5637
17. Stoica GE, Kuo A, Aigner A, Sunitha I, Soultou B, Malerczyk C, Caughey DJ, Wen D, Karavanov A, Riegel AT, Wellstein A: Identification of anaplastic lymphoma kinase as a receptor for the growth factor pleiotrophin. *J Biol Chem* 2001, 276:16772-16779
18. Stoica GE, Kuo A, Powers C, Bowden ET, Sale EB, Riegel AT, Wellstein A: Midkine binds to anaplastic lymphoma kinase (ALK) and acts as a growth factor for different cell types. *J Biol Chem* 2002, 277:35990-35998
19. Evans AE, D'Angio GJ, Randolph J: A proposed staging for children with neuroblastoma: children's cancer study group A. *Cancer* 1971, 27:374-378
20. Nakagawara A, Arima-Nakagawara M, Scavarda NJ, Azar CG, Cantor AB, Brodeur GM: Association between high levels of expression of the TRK gene and favorable outcome in human neuroblastoma. *N Engl J Med* 1993, 328:847-854
21. Nakagawara A, Azar CG, Scavarda NJ, Brodeur GM: Expression and function of TRK-B and BDNF in human neuroblastomas. *Mol Cell Biol* 1994, 14:759-767
22. Nakagawara A, Nakamura Y, Ikeda H, Hiwasa T, Kuida K, Su MS, Zhao H, Cnaan A, Sakiyama S: High levels of expression and nuclear localization of interleukin-1 beta converting enzyme (ICE) and CPP32 in favorable human neuroblastomas. *Cancer Res* 1997, 57:4578-4584
23. Posmantur R, McGinnis K, Nadimpalli R, Gilbertsen RB, Wang K: Characterization of CPP32-like protease activity following apoptotic challenge in SH-SY5Y neuroblastoma cells. *J Neurochem* 1997, 68:2328-2337
24. Adida C, Berrebi D, Peuchmaur M, Reyes-Mugica M, Altieri DC: Anti-apoptosis gene, survivin, and prognosis of neuroblastoma. *Lancet* 1998, 351:882-883
25. Hiyama E, Hiyama K, Yokoyama T, Matsuura Y, Pratsyzek MA, Shay JW: Correlating telomerase activity levels with human neuroblastoma outcomes. *Nat Med* 1995, 1:249-255
26. Lamant L, Pulford K, Bischof D, Morris SW, Mason DY, Delsol G, Mariame B: Expression of the ALK tyrosine kinase gene in neuroblastoma. *Am J Pathol* 2000, 156:1711-1721
27. Miyake I, Hakomori Y, Shinohara A, Gamou T, Saito M, Iwamatsu A, Sakai R: Activation of anaplastic lymphoma kinase is responsible for hyperphosphorylation of ShcC in neuroblastoma cell lines. *Oncogene* 2002, 21:5823-5834
28. Sakai R, Henderson JT, O'Bryan JP, Elia AJ, Saxton TM, Pawson T: The mammalian ShcB and ShcC phosphotyrosine docking proteins function in the maturation of sensory and sympathetic neurons. *Neuron* 2000, 28:819-833
29. Perucho M, Goldfarb M, Shimizu K, Lama C, Fogh J, Wigler M: Human-tumor-derived cell lines contain common and different transforming genes. *Cell* 1981, 27:467-476
30. Brodeur GM, Pritchard J, Berthold F, Carlsen NL, Castel V, Castellberry RP, De Bernardi B, Evans AE, Favrot M, Hedborg F, Kaneko M, Kemshead J, Lampert F, Lee RE, Look AT, Pearson AD, Philip T, Roald B, Sawada T, Seeger RC, Tsuchida Y, Voute PA: Revisions of the international criteria for neuroblastoma diagnosis, staging, and response to treatment. *J Clin Oncol* 1993, 11:1466-1477
31. Shimada H, Ambros IM, Dehner LP, Hata J, Joshi VV, Roald B, Stram DO, Gerbing RB, Lukens JN, Matthay KK, Castleberry RP: The International Neuroblastoma Pathology Classification (the Shimada system). *Cancer* 1999, 86:364-372
32. Ikeda I, Ishizaka Y, Tahira T, Suzuki T, Onda M, Sugimura T, Nagao M: Specific expression of the ret proto-oncogene in human neuroblastoma cell lines. *Oncogene* 1990, 5:1291-1296
33. Motegi A, Fujimoto J, Kotani M, Sakuraba H, Yamamoto T: ALK receptor tyrosine kinase promotes cell growth and neurite outgrowth. *J Cell Sci* 2004, 117:3319-3329
34. Slamon DJ, Clark GM, Wong SG, Levin WJ, Ullrich A, McGuire WL: Human breast cancer: correlation of relapse and survival with amplification of the HER-2/neu oncogene. *Science* 1987, 235:177-182
35. Tsuda H, Hirohashi S, Shimosato Y, Hirota T, Tsugane S, Yamamoto H, Miyajima N, Toyoshima K, Yamamoto T, Yokota J, Yoshida T, Sakamoto H, Terada M, Sugimura T: Correlation between long-term survival in breast cancer patients and amplification of two putative oncogene-coamplification units: hst-1/int-2 and c-erbB-2/ear-1. *Cancer Res* 1989, 49:3104-3108
36. Ganju P, O'Bryan JP, Der C, Winter J, James IF: Differential regulation of SHC proteins by nerve growth factor in sensory neurons and PC12 cells. *Eur J Neurosci* 1998, 10:1995-2008
37. Nakamura T, Komiya M, Gotoh N, Koizumi S, Shibuya M, Mori N: Discrimination between phosphotyrosine-mediated signaling properties of conventional and neuronal Shc adapter molecules. *Oncogene* 2002, 21:22-31
38. Nakamura T, Muraoka S, Sanokawa R, Mori N: N-Shc and Sck, two neuronally expressed Shc adapter homologs: their differential regional expression in the brain and roles in neurotrophin and Src signaling. *J Biol Chem* 1998, 273:6960-6967
39. O'Bryan JP, Songyang Z, Cantley L, Der CJ, Pawson T: A mammalian adaptor protein with conserved Src homology 2 and phosphotyrosine-binding domains is related to Shc and is specifically expressed in the brain. *Proc Natl Acad Sci USA* 1996, 93:2729-2734
40. Pellicci G, Troglio F, Bodini A, Melillo RM, Pettirossi V, Coda L, De Giuseppe A, Santoro M, Pellicci PG: The neuron-specific Rai (ShcC) adaptor protein inhibits apoptosis by coupling Ret to the phosphatidylinositol 3-kinase/Akt signaling pathway. *Mol Cell Biol* 2002, 22:7351-7363
41. Yuan J, Yankner BA: Apoptosis in the nervous system. *Nature* 2000, 407:802-809
42. De Vita G, Melillo RM, Carlomagno F, Visconti R, Castellone MD, Bellacosa A, Billaud M, Fusco A, Tschlis PN, Santoro M: Tyrosine 1062 of RET-MEN2A mediates activation of Akt (protein kinase B) and mitogen-activated protein kinase pathways leading to PC12 cell survival. *Cancer Res* 2000, 60:3727-3731

LMO3 Interacts with Neuronal Transcription Factor, HEN2, and Acts as an Oncogene in Neuroblastoma

Mineyoshi Aoyama,¹ Toshinori Ozaki,¹ Hiroyuki Inuzuka,¹ Daihachiro Tomotsune,³ Junko Hirato,⁴ Yoshiaki Okamoto,¹ Hisashi Tokita,² Miki Ohira,¹ and Akira Nakagawara¹

Divisions of ¹Biochemistry and ²Animal Science, Chiba Cancer Center Research Institute; ³Center for Functional Genomics, Hisamitsu Pharmaceutical Co., Inc., Chiba, Japan and ⁴Department of Pathology, Gunma University School of Medicine, Gunma, Japan

Abstract

LIM-only proteins (LMO), which consist of LMO1, LMO2, LMO3, and LMO4, are involved in cell fate determination and differentiation during embryonic development. Accumulating evidence suggests that LMO1 and LMO2 act as oncogenic proteins in T-cell acute lymphoblastic leukemia, whereas LMO4 has recently been implicated in the genesis of breast cancer. However, little is known about the role of LMO3 in either tumorigenesis or development. In the present study, we have identified *LMO3* and *HEN2*, which encodes a neuronal basic helix-loop-helix protein, as genes whose expression levels were higher in unfavorable neuroblastomas compared with those of favorable tumors. Immunoprecipitation and immunostaining experiments showed that LMO3 was associated with HEN2 in mammalian cell nucleus. Human neuroblastoma SH-SY5Y cells stably overexpressing LMO3 showed a marked increase in cell growth, a promotion of colony formation in soft agar medium, and a rapid tumor growth in nude mice compared with the control transfectants. More importantly, the increased expression of LMO3 and HEN2 was significantly associated with a poor prognosis in 87 primary neuroblastomas. These results suggest that the deregulated expression of neuronal-specific LMO3 and HEN2 contributes to the genesis and progression of human neuroblastoma in a lineage-specific manner. (Cancer Res 2005; 65(11): 4587-97)

Introduction

The LIM domain-containing proteins are important regulators in determining cell fate and controlling cell growth and differentiation during embryonic development (1). The LIM domain is a highly conserved cysteine-rich zinc finger-like motif found in a variety of nuclear and cytoplasmic proteins and acts as a docking site for the assembly of multiprotein complexes (2-4). However, the precise role of the LIM domain is still unclear. Several distinct subgroups of the LIM domain-containing proteins are defined and some of them also possess a functionally divergent domain, including a DNA-binding homeodomain or a protein kinase domain (1, 2).

The LIM-only proteins (LMO) are one of the families of the LIM domain-containing proteins and possess only two tandem LIM domains. They consist of four members, including LMO1, LMO2, LMO3, and LMO4 (2, 4). *LMO1* and *LMO2* have been identified as the genes that are activated in human acute T-cell leukemia (T-cell ALL) by tumor-specific chromosomal trans-

locations (4). Transgenic mice overexpressing LMO1 or LMO2 developed immature and aggressive T-cell leukemia, suggesting that these proteins act as T-cell oncoproteins (5-7). On the other hand, LMO4 has been identified as a nuclear protein that interacts with the adaptor protein Ldb1 (8). It has been shown recently that LMO4 is highly expressed in primary human breast cancers, and overexpression of LMO4 inhibits differentiation of mammary epithelial cells, suggesting that deregulated expression of LMO4 contributes to the breast carcinogenesis (9). LMO4 has also been reported to be associated with BRCA1 to repress its transcriptional activity (10). Thus, LMO1, LMO2, and LMO4 have been implicated in tumorigenesis. However, to date, little is known about the oncogenic function of LMO3, which has been discovered based on sequence homology with LMO1 (11).

The nuclear LMO proteins, which lack intrinsic DNA-binding activity, have been considered to be involved in transcriptional regulation (2), raising a possibility that they alter the transcription of target genes by forming a complex with other transcription factors with DNA-binding activity. Indeed, in T-cell acute lymphoblastic leukemia in children, a basic helix-loop-helix transcription factor, TAL1, is physically associated with LMO1 or LMO2 and enhances their oncogenic activities (12, 13). Interestingly, the neuronal-specific basic helix-loop-helix transcription factors, HEN1 and HEN2, were identified based on cross-hybridization with TAL1 (14, 15). Their expression was restricted to the developing nervous system and a human neuroblastoma cell line. However, the role of HEN1 and HEN2 in tumorigenesis has long been elusive.

Neuroblastoma is one of the most common childhood cancers and is originated from sympathoadrenal lineage of the neural crest (16). It is clinically and cytogenetically divided into two major subgroups with favorable and unfavorable prognosis (17). The recent molecular and cellular analyses have revealed that amplification of *MYCN* and *DDX1* as well as loss of heterozygosity at the region of chromosome 1p36 are strongly associated with a poor outcome, whereas high levels of expression of the neurotrophin receptors *TrkA*, *CD44*, and *Fyn*, are well correlated with favorable prognosis (16-23). However, we still do not know many other genes that play important roles in the genesis and progression of neuroblastoma. To identify the other genes closely involved in neuroblastoma, we have constructed several cDNA libraries from different subsets of neuroblastoma and randomly cloned 4,200 genes (24). Screening of the genes differentially expressed between favorable and unfavorable subsets of the tumor has identified *Nbla3267* as one of the genes expressed at higher levels in unfavorable than favorable neuroblastomas (25).

In the present study, we found that *Nbla3267* encoded the human LMO, LMO3, and that high expression of *LMO3* as well as *HEN2* was strongly associated with a poor prognosis of neuroblastoma. Furthermore, LMO3 interacted with HEN2 in mammalian

Requests for reprints: Akira Nakagawara, Division of Biochemistry, Chiba Cancer Center Research Institute, 666-2 Nitona, Chuoh-ku, Chiba 260-8717, Japan. Phone: 81-43-264-5431; Fax 81-43-265-4459; E-mail: akiranak@chiba-cc.jp.
©2005 American Association for Cancer Research.

cell nucleus, and enforced expression of LMO3 in human neuroblastoma-derived cell line SH-SY5Y markedly enhanced tumor growth in nude mice, supporting the oncogenic role of LMO3 in neuroblastoma.

Materials and Methods

Patient population. The RNA samples obtained from 87 patients with neuroblastoma were subjected to semiquantitative and quantitative real-time reverse transcription-PCR (RT-PCR) analyses. All patients were diagnosed clinically as well as pathologically and tested for DNA ploidy, MYCN amplification, and TrkA expression. Tumors were staged according to the International Neuroblastoma Staging System criteria (26). Thirty-four patients were stage I, 14 were stage II, 8 were stage III, 26 were stage IV, and 5 were stage IVS. Stages I, II, and IVS were considered as favorable and stages III and IV as unfavorable. The patients were treated following the protocols proposed by the Japanese Infantile Neuroblastoma Cooperative Study (27) and the Study Group of Japan for Treatment of Advanced Neuroblastoma (28). The clinical follow-up ranged from 4 to 58 months, with a median of 36 months. We have a precise list of patient characteristics, including age, stage, and clinical follow-up time, and this list will be provided upon request.

Cloning of human LMO3, HEN1, and HEN2. To obtain a complete human LMO3 cDNA, a cDNA library derived from human fetal brain (Stratagene, La Jolla, CA) was screened with a ³²P-labeled *Nbla3267* cDNA. Plaques showing positive signals were picked up and rescreened twice. To construct the expression plasmid for hemagglutinin (HA)-tagged LMO3-A, the cDNA fragment encoding the entire LMO3-A protein was amplified by PCR from the phage clone as a template using the primers designed to add a synthetic linker encoding the HA epitope on the NH₂-terminal side of LMO3-A (forward 5'-GGTACCATTGGCTTACCCATACGATGTTCCAGATTACGCTAGCCTCTCAGTCCAGCCAGACAC-3' and reverse 5'-TCAGATATCATTAGATCAGCGAACCTGGG-3'). The PCR product was digested with *KpnI* and *EcoRV* and subcloned into the identical restriction sites of pcDNA3 expression plasmid to give pcDNA3-HA-LMO3-A. cDNA encoding human HEN1 (amino acid residues 1-133) or HEN2 (amino acid residues 1-135) was generated by reverse transcribing total RNA isolated from neuroblastoma cell line, IMR32, using a forward primer (5'-AAGGAATTCATGCTCAACTCAGACACCATG-3') and a reverse primer (5'-ATAAGAATGCGCCGCTCAGACAGT-3') for HEN1 and a forward primer (5'-AAGGAATTCATGCTGAGTCCGGACCAAGCA-3') and a reverse primer (5'-ATAAGAATGCGCCGCTACAGTCCAGGACGTGGT-3') for HEN2. The amplified PCR products were digested with *EcoRI* and *NotI* and subcloned into the identical restriction sites of pcDNA3-FLAG expression plasmid to give pcDNA-FLAG-HEN1 and pcDNA3-FLAG-HEN2.

Generation of a polyclonal anti-LMO3 antibody. The polyclonal anti-LMO3 and anti-HEN2 antibodies were raised against a peptide "Cys" plus containing the amino acid sequence between positions 127 and 145 of LMO3 and the amino acid sequence between positions 1 and 19 of HEN2, respectively. The peptides and the polyclonal antibodies were produced by Biologica Co. (Nagoya, Japan).

Cell culture and transfection. Human neuroblastoma (SK-N-AS, SH-SY5Y, NB69, OAN, SK-N-BE, NGP, NLF, IMR32, NB1, and KP-N-NS), ALL (RPMI, KOPT, HSB, and MOLT), osteosarcoma (OST, SAOS-2, and U2OS), rhabdomyosarcoma (RMS-MK), colon cancer (COLO-320), breast cancer (MCF-7 and MDA-MB-453), melanoma (G361, G32TG, and A875), thyroid cancer (TTC11), small cell lung carcinoma (H1299), and cervical cancer (HeLa) cell lines and COS7 cells were maintained in RPMI 1640 or DMEM supplemented with 10% heat-inactivated fetal bovine serum (FBS), 100 IU/mL penicillin, and 100 µg/mL streptomycin at 37°C in an atmosphere of 5% CO₂ in the air. For transient transfection, COS7 cells were transfected with the indicated expression plasmids using FuGene 6 transfection reagent as recommended by the manufacturer (Roche Molecular Biochemicals, Mannheim, Germany). Stable transfections of SH-SY5Y cells were done with the empty plasmid (pcDNA3, Invitrogen, Carlsbad, CA) or with the expression plasmid for FLAG-tagged LMO3-A using LipofectAMINE Plus transfection reagent according to the manufacturer's

instructions (Invitrogen). The transfected cells were cultured in the presence of G418 at a final concentration of 400 µg/mL (Sigma Chemical Co., St. Louis, MO). Thereafter, the selection medium was replaced every 3 days. Three weeks after the selection in G418, drug-resistant clones were isolated and allowed to proliferate in medium containing G418.

Reverse transcription-PCR analysis. Total RNA was prepared from cultured cells and human tissues by using Trizol reagent (Life Technologies, Grand Island, NY) or the RNeasy Mini kit (Qiagen, Valencia, CA). Reverse transcription was carried out using random primers and SuperScript II (Invitrogen). Following the reverse transcription, the resultant cDNA was subjected to PCR-based amplification. Oligonucleotides used to amplify LMO3-A, LMO3-B, LMO1, LMO2, LMO4, *Ldb1*, *Ldb2*, *TAL1*, *HEN1*, *HEN2*, and glyceraldehyde-3-phosphate dehydrogenase (*GAPDH*) mRNAs were as follows: LMO3-A: forward 5'-ACTGTGCTACTGAACGGCCTC-3' and reverse 5'-CCGGTCTTGATCTTTCGGTTG-3'; LMO3-B: forward 5'-TGCAACTCAGACAGCCTAAG-3' and reverse 5'-CCGGTCTTGATCTTTCGGTTG-3'; LMO1: forward 5'-GCTCCACCCTCTACACCAAG-3' and reverse 5'-CTGCCCTTCTCATAGTCCA-3'; LMO2: forward 5'-AATGCGGGTGAAGACAAAG-3' and reverse 5'-CCCCAAGTGCCTAAGAGTG-3'; LMO4: forward 5'-GCAAGGCAATGTGTATCATCT-3' and reverse 5'-GCATTCTGCAT-TACTCTGACC-3'; *Ldb1*: forward 5'-CCAGGGGACAGAAGACAGAA-3' and reverse 5'-AGAGGCCAGGTTCCAAG-3'; *Ldb2*: forward 5'-TAGCCCAAGTGTGAAACAA-3' and reverse 5'-TAACTGCCACAAAACAA-3'; *TAL1*: forward 5'-GTTCTTAGGCTGCTGGGATG-3' and reverse 5'-GATTTGGGACTGAGGGAAGA-3'; *HEN1*: forward 5'-AGAGACTGAGTCGGGCTTCA-3' and reverse 5'-CAGGGCAGAATCTCAATCT-3'; *HEN2*: forward 5'-CCCCAAGGGTGTGGTTTA-3' and reverse 5'-TCTGAATCTGCCCCT-CATTCTTT-3'; and *GAPDH*: forward 5'-ACCTGACCTGCCGTCTAGAA-3' and reverse 5'-TCCACCACCTGTGCTGTA-3'. Amplified products were electrophoretically separated on agarose gels and visualized by ethidium bromide staining. The gels were photographed under UV illumination.

Northern analysis. A human MTN blot (Clontech, Palo Alto, CA), a nylon membrane on which poly(A)⁺ RNAs extracted from various human normal tissues were blotted, was used for analysis of the distribution of LMO3 expression in human normal tissues. ³²P-labeled probe was prepared by random priming of the 2.5-kb restriction fragment of LMO3 cDNA. The membrane was hybridized overnight at 65°C in a solution containing 7.5% dextran sulfate, 1 mol/L NaCl, 1% *N*-lauryl sarcosine, 100 µg/mL heat-denatured salmon sperm DNA, and the radiolabeled probe. The membrane was washed twice in 0.5 × SSC/0.1% *N*-lauryl sarcosine at 50°C. Specific signals were obtained by autoradiography.

Section in situ hybridization. Section *in situ* hybridization was done as described previously (29). A riboprobe was synthesized with digoxigenin-UTP and T3 or T7 polymerase (Roche Molecular Biochemicals). The alkaline phosphatase reaction was done with nitroblue tetrazolium/5-bromo-4-chloro-3-indolyl phosphate (Roche Molecular Biochemicals). The riboprobe used for the section *in situ* hybridization were transcripts of the human cDNA fragments of the LMO3 gene.

Immunohistochemistry. Neuroblastoma tissues were stained with immunoperoxidase method using anti-HEN2 antibody. They included unfavorable neuroblastomas with MYCN gene amplification and favorable neuroblastomas with a single copy of MYCN gene. Neuroblastoma specimens were fixed in 10% buffered formalin and embedded in paraffin, and 3 µm sections were applied to the immunostaining. Before incubation with anti-HEN2 antibody, the sections were treated with 0.05% Pronase in 0.05 mol/L Tris-HCl (pH 7.6) for 5 minutes. The sections were incubated with anti-HEN2 antibody, which was diluted to 1:200 at 4°C overnight. The biotin-streptavidin method (Nichirei, Tokyo, Japan) was done, and the sections were visualized with diaminobenzidine solution. The nuclei were counterstained with hematoxylin.

Immunofluorescent staining. COS7 cells were doubly transfected with the expression plasmids for HA-LMO3-A and FLAG-HEN2. Forty-eight hours after transfection, cells were fixed for 30 minutes with 3.7% formaldehyde in PBS and permeabilized with 0.2% Triton X-100 for 5 minutes, and nonspecific epitopes were blocked for 1 hour in PBS containing 3% bovine serum albumin. The cells were then incubated with a polyclonal anti-HA antibody (1:200 dilution, Medical and Biological Laboratories, Nagoya,

Japan) and a monoclonal anti-FLAG antibody (1:50, M2, Sigma Chemical). After three washes with PBS, cells were stained with a FITC- or a rhodamine-conjugated secondary antibody (1:200, Invitrogen). The coverslips were mounted onto glass slides, and the stained cells were viewed using a confocal laser scanning microscope (Olympus, Tokyo, Japan).

Western blot analysis and immunoprecipitation. After transfection, cells were rinsed twice with ice-cold PBS and then lysed immediately with SDS sample buffer. Equal amounts of proteins were separated under denaturing conditions by electrophoresis in 15% polyacrylamide gel containing SDS-PAGE and electrotransferred to polyvinylidene difluoride membrane (Immobilon-P, Millipore, Bedford, MA). After blocking in a solution containing 5% skim milk, the membrane was incubated with a monoclonal anti-FLAG, a polyclonal anti-HA, a polyclonal anti-LMO3, or a polyclonal anti-actin antibody (20-33, Sigma Chemical) and then incubated with a horseradish peroxidase-conjugated goat anti-mouse or anti-rabbit secondary antibody (Jackson ImmunoResearch Laboratories, West Grove, PA). Protein bands were visualized with an enhanced chemiluminescence (Amersham Pharmacia Biotech, Piscataway, NJ). For immunoprecipitation, transfected cells were lysed in EBC buffer [50 mmol/L Tris-HCl (pH 7.5), 120 mmol/L NaCl, 0.5% NP40, 1 mmol/L phenylmethylsulfonyl fluoride] containing protease inhibitor mixture (Sigma Chemical). The precleared soluble supernatants were mixed with a polyclonal anti-HA or a monoclonal anti-FLAG antibody and incubated for 2 hours at 4°C. Protein A-Sepharose

beads were then added to the reaction mixtures and incubated for 1 hour at 4°C. The immune complexes were washed with the lysis buffer thrice at 4°C. The bound proteins were resuspended in SDS sample buffer, resolved by SDS-PAGE, and analyzed by Western blotting.

Cell proliferation and soft agar assay. Cells were seeded in triplicate in 24-well plates (5×10^3 per well) in culture medium containing 10% or 1% FBS. Cells were allowed to adhere to the bottom of the cell culture dish for 24 hours. At the indicated times, cells were trypsinized and cell counting was carried out using a Coulter Counter (Coulter Electronics Ltd., Hiialeah, Finland). For soft agar assay, 2.5×10^3 cells of the stable transfectants or the parental SH-SY5Y cells were seeded in triplicate in 35-mm cell culture plates containing 0.2% agar and RPMI 1640 supplemented with 10% FBS. After 21 days, colonies with diameters $>300 \mu\text{m}$ were scored as positive.

Tumor formation in nude mice. For tumor formation, 6-week-old female athymic *nu/nu* mice (Charles River Laboratory, Sulzfeld, Germany) were injected into the femur with 5×10^6 parental SH-SY5Y cells or SH-SY5Y cells transfected with the empty plasmid or with the expression plasmid encoding LMO3-A suspended in 100 μL PBS. Tumor size and body weight were measured once weekly and mice were sacrificed 7 weeks after injection. For histologic examinations, tumor tissues were fixed in fresh 10% buffered formalin and embedded in paraffin. The handling of animals was in accordance with the guidelines of the Chiba Cancer Center Research Institute (Chiba, Japan).

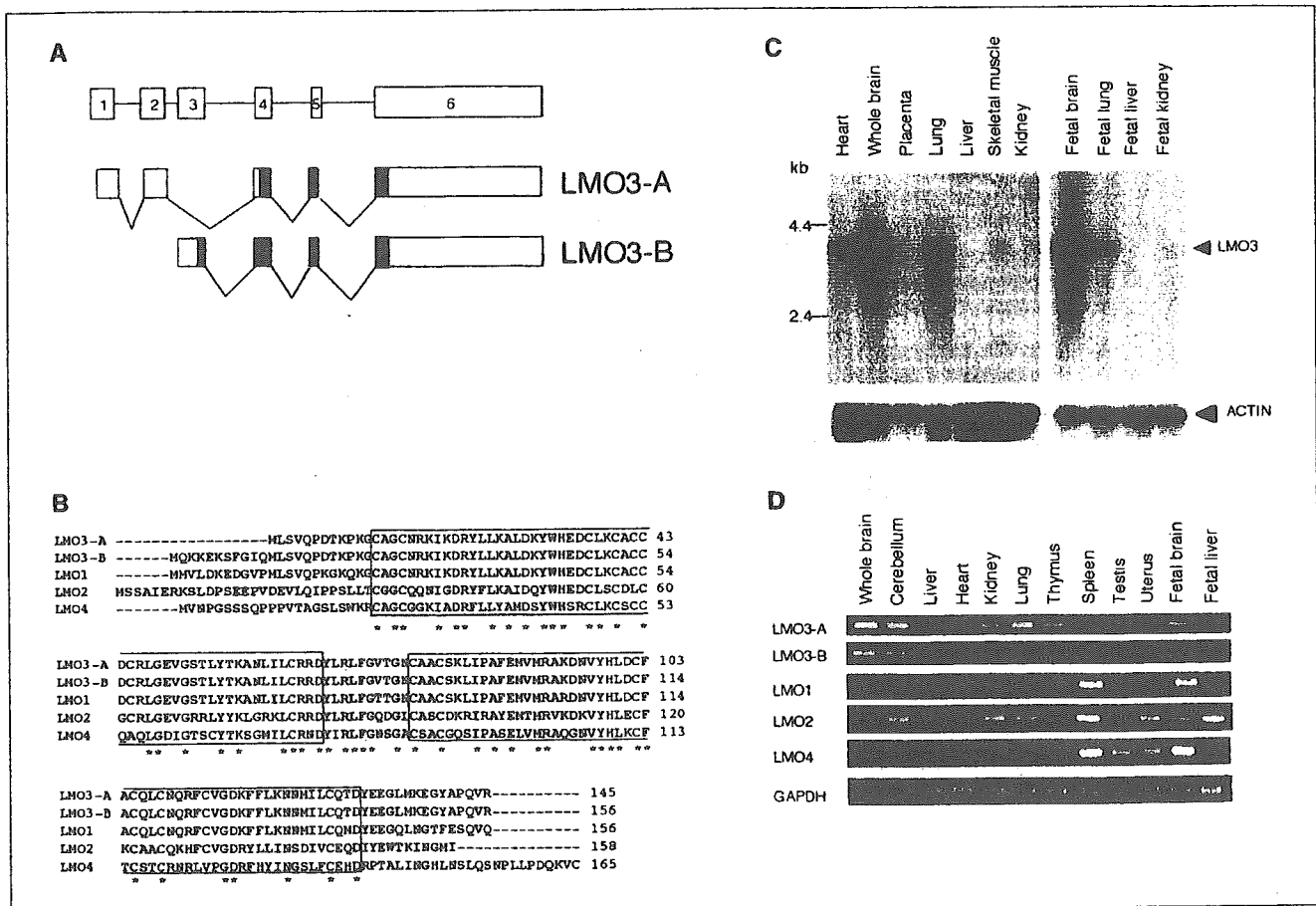


Figure 1. Identification of human LMO3-A and LMO3-B and their relation to the other LMO family members. *A*, schematic representation of the exons of human LMO3 gene. *Solid* and *open boxes*, coding and untranslated regions, respectively. *B*, deduced amino acid sequences of human LMO3-A and LMO3-B and their alignments with those of human LMO1, LMO2, and LMO4. *Asterisks*, identical amino acid residues. Two LIM domains are *boxed*. *C*, tissue-specific expression of LMO3. Human multiple tissue Northern blots containing poly(A)⁺ RNA were hybridized with a radiolabeled human LMO3 cDNA (*top*) or with a radioactive probe derived from human β -actin cDNA (*bottom*). β -actin was used as a control for equal loading. The 2-kb band was hybridized ubiquitously, and an additional 1.8-kb band was hybridized in heart and skeletal muscle with the β -actin probe. *D*, coordinated expression of LMO3-A and LMO3-B in various human tissues. Total RNA isolated from the indicated human tissues was subjected to RT-PCR analysis to examine the expression levels of LMO3-A, LMO3-B, LMO1, LMO2, and LMO4. GAPDH expression is shown as an internal control.

Quantitative real-time PCR. Total RNA prepared from primary neuroblastomas was reverse transcribed into cDNA (SuperScript II kit) and subjected to the real-time PCR. The expression level of *GAPDH* was measured in all samples to normalize *LMO3* and *HEN2* expression according to the manufacturer's instructions (Applied Biosystems, Foster City, CA). Oligonucleotide primers and TaqMan probes, which were labeled at the 5' end with the reporter dye 6-carboxyfluorescein (FAM) and at the 3' end with the quencher dye 6-carboxytetramethylrhodamine (TAMRA), were as follows: *LMO3*: forward 5'-TCTGAGGCTCTT-TGGTGTAAACG-3', reverse 5'-CCAGGTGGTAAACATTGTCCTTG-3', and probe 5'-FAM-AAACTGCGCTGCCTGTAGTAAGCTCATCC-TAMRA-3' and *HEN2*: forward 5'-CCCAAGGTTGTGGTTTA-3', reverse 5'-TCTGAACCTCTGCCCTCATCTTT-3', and probe 5'-FAM-TTGAGTTCTCC-TACATTCATCCGCCACAA-TAMRA-3'. Amplification and detection were done using the ABI Prism 7700 Sequence Detection System (Applied Biosystems).

Statistical analysis. Student's *t* tests were used to explore possible associations between *LMO3* expression and other factors. Because the values of the *LMO3* expression were skewed, a log transformation was used to achieve the normality in the analyses using *t* test and Cox regression. The distinction between high and low levels of *LMO3* expression was based on the median value (low, *LMO3* < 0.2493 e.u.; high, *LMO3* > 0.2493 e.u.) regardless of tumor stage, *MYCN* copy number, or survival. The distinction between high and low levels of *HEN2* expression was based on the distribution of the values (low, undetectable; high, detectable). χ^2 tests were

used to examine possible associations between *HEN2* expression and other factors, such as tumor stage. Kaplan-Meier survival curves were calculated, and survival distributions were compared using the log-rank test. Cox regression models were used to explore associations among *LMO3* expression, *HEN2* expression, age, *MYCN* amplification, mass screening, origin, and survival. Statistical significance was declared if *P* < 0.05. The statistical analysis was done using Stata Statistical Software Release 7.0 (Stata Corp., College Station, TX, 2001).

Results

Identification of the human *LMO3* gene. To identify the genes specifically involved in the genesis and progression of neuroblastoma, we have previously constructed cDNA libraries from the primary neuroblastomas and screened for the differentially expressed genes between the tumors with good and poor clinical outcome (25). One of the cDNA clones, *Nbla3267*, significantly overexpressed in the poor prognostic neuroblastomas contained a partial nucleotide sequence encoding a LMO family protein, LMO3. To obtain the missing 5' part of the *LMO3* cDNA, we screened a cDNA library derived from human fetal brain. From ~6 × 10⁵ recombinant phage clones, 10 independent phage clones were isolated. Sequence analysis

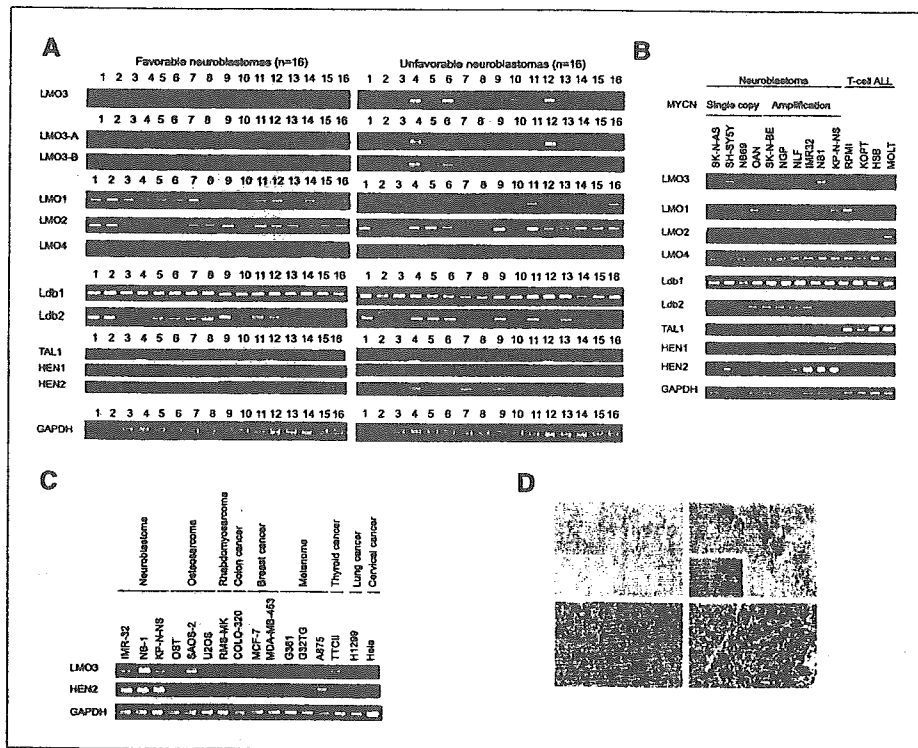


Figure 2. Increased expression of *LMO3* and *HEN2* in unfavorable neuroblastomas and neuroblastoma-derived cell lines. **A**, expression of *LMO3* and *LMO*-related genes in primary neuroblastomas with favorable (stage I, a single copy of *MYCN* and high expression of *TrkA*) and unfavorable (stages III and IV, *MYCN* amplification and decreased expression of *TrkA*) characteristics. Total RNA was isolated from the indicated neuroblastoma tissues, reverse transcribed, and amplified by PCR to examine the expression levels of *LMO3*, *LMO3-A*, *LMO3-B*, *LMO1*, *LMO2*, *LMO4*, *Ldb1*, *Ldb2*, *TAL1*, *HEN1*, and *HEN2*. Expression of *GAPDH* serves as an internal control. PCR products were visualized by ethidium bromide staining. **B**, expression of *LMO3* and *LMO*-related genes in neuroblastoma cell lines without *MYCN* amplification (SK-N-AS, SH-SY5Y, NB69, and OAN), neuroblastoma cell lines with *MYCN* amplification (SK-N-BE, NGP, NLF, IMR32, NB1, and KP-N-NS), and ALL cell lines (RPMI, KOPT, HSB, and MOLT). Total RNA prepared from the indicated cultured cells was subjected to RT-PCR analysis. Expression of *GAPDH* serves as an internal control. **C**, expression of *LMO3* and *HEN2* in various tumor-derived cell lines. Total RNA prepared from the indicated culture cells was subjected to RT-PCR analysis as described above. **D**, section *in situ* hybridization of neuroblastoma with the *LMO3* probe. Serial sections of the favorable neuroblastoma tissue (top left and inset) or the unfavorable one with *MYCN* amplification (top right and inset) were prepared, and expression of the *LMO3* gene was examined by section *in situ* hybridization. The *LMO3* transcripts are positive in unfavorable neuroblastoma. Immunohistochemical staining of *HEN2* in primary neuroblastoma tissues. *HEN2* is strongly positive in the nucleus of most tumor cells with *MYCN* amplification (bottom right), whereas it is negative in the favorable neuroblastoma tissue (bottom left).

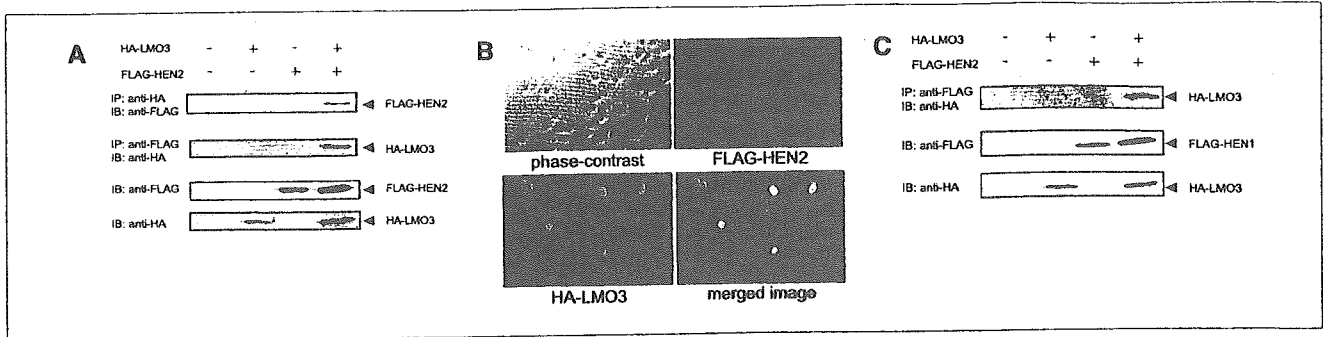
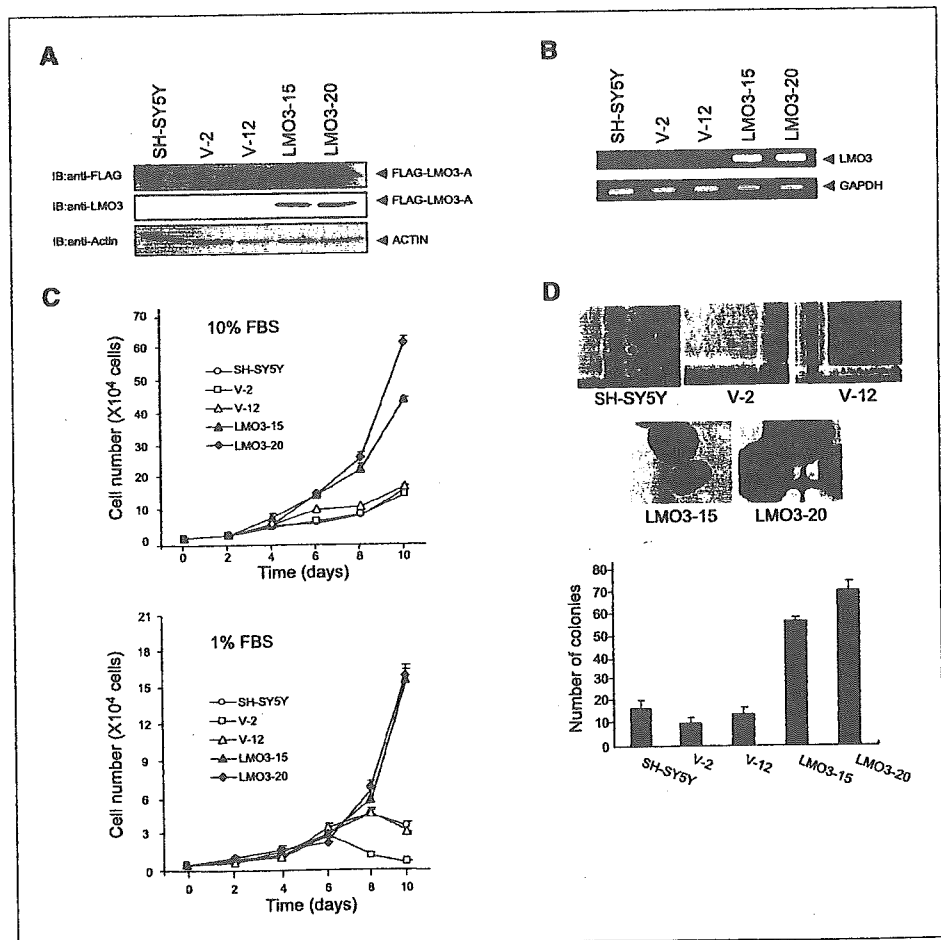


Figure 3. LMO3 interacts with HEN2 in mammalian cells. **A**, coimmunoprecipitation analysis. COS7 cells were transfected with the indicated expression plasmids. Forty-eight hours after transfection, whole cell lysates were prepared and subjected to the immunoprecipitation/Western analysis (*top* and *top middle*). Whole cell lysates were monitored on immunoblot for the expression of FLAG-HEN2 (*bottom middle*) and HA-LMO3-A (*bottom*). **B**, nuclear colocalization of LMO3 and HEN2 in cultured cells. COS7 cells were cotransfected with the expression plasmids for HA-LMO3-A and FLAG-HEN2. Forty-eight hours after transfection, cells were fixed and incubated with the polyclonal anti-HA and monoclonal anti-FLAG antibodies. Cells were then processed for double immunofluorescence using the FITC-conjugated anti-rabbit IgG (*green*) and with the rhodamine-conjugated anti-mouse IgG (*red*). The merged images (*yellow*) suggest the nuclear colocalization of LMO3 and HEN2. The phase-contrast images are also shown. **C**, coimmunoprecipitation of FLAG-HEN1 and HA-LMO3. Whole cell lysates prepared from COS7 cells transfected with the indicated combinations of the expression plasmids were immunoprecipitated with the anti-FLAG antibody followed by immunoblotting with the anti-HA antibody (*top*). Levels of FLAG-HEN1 and HA-LMO3 were also examined by immunoblotting with the anti-FLAG antibody (*middle*) and with the anti-HA antibody (*bottom*), respectively.

revealed that they were divided into two types, designated LMO3-A (145 amino acids) and LMO3-B (156 amino acids), with the different translation initiation sites. The NH₂-terminal region of LMO3-A was identical to that of the previously reported

LMO3 protein (11). As shown in Fig. 1A, the putative translation initiation sites of LMO3-A and LMO3-B were located within exons 4 and 3, respectively. Because LMO3 is a single gene, it is likely that LMO3-A and LMO3-B arise from differential splicing

Figure 4. Growth-promoting activity of LMO3 in SH-SY5Y cells. **A**, stable SH-SY5Y transfectants expressing exogenous FLAG-LMO3-A. SH-SY5Y cells were stably transfected with the empty plasmid or with the expression plasmid for FLAG-LMO3-A and maintained in the presence of G418 (at a final concentration of 400 μg/mL) for 3 weeks. Whole cell lysates prepared from the indicated drug-resistant cell clones in addition to the parental SH-SY5Y cells were subjected to Western blot analysis using the anti-FLAG (*top*), anti-LMO3 (*middle*), or anti-actin (*bottom*) antibody. **B**, RT-PCR analysis of LMO3 in the indicated stable transfectants along with the parental SH-SY5Y cells. Expression of GAPDH serves as an internal control. **C**, effects of LMO3 overexpression on cell growth in SH-SY5Y cells. SH-SY5Y cells and the indicated transfectants were grown in the culture medium containing 10% (*top*) or 1% (*bottom*) FBS. Cells were harvested at 48-hour time intervals and number of cells was counted in triplicate. *Points*, means from three independent experiments; *bars*, SE. **D**, anchorage-independent growth of LMO3-overexpressing transfectants. The parental SH-SY5Y cells and the indicated transfectants (2.5×10^3 cells per dish) were grown in soft agar medium. After 3 weeks of culture, cells were examined by phase-contrast microscopy (*top*), and the numbers of colonies with a diameter of >300 μm were counted (*bottom*). *Columns*, means from three independent experiments; *bars*, SE.



or alternative promoter usage. Amino acid sequence alignment of LMO3 with the other LMO family proteins (LMO1, LMO2, and LMO4) showed a significant homology among them (Fig. 1B). LIM domains of LMO3 presented 98%, 60%, and 55% amino acid homology with those of LMO1, LMO2, and LMO4, respectively.

To determine the expression pattern of human *LMO3* mRNA, we did Northern blot analysis on a human multiple tissues blot using β -actin as a control. As shown in Fig. 1C, *LMO3* mRNA (~4 kb) was abundantly expressed in brain and at relatively low levels in the heart and lung but not in the other tissues examined. Similar to the adult tissues, *LMO3* mRNA was expressed predominantly in fetal brain, with a lower level in fetal lung. We then compared the tissue distribution of *LMO3-A* expression with those of *LMO3-B* and the other *LMO* family gene expression in various human adult and fetal tissues by RT-PCR (Fig. 1D). The expression pattern of *LMO3-A* was similar to that of *LMO3-B*, with relatively higher levels in brain, cerebellum, and fetal brain. In contrast, *LMO2* and *LMO4* were expressed ubiquitously in human tissues, and *LMO1* was expressed at higher levels in spleen and fetal brain.

Expression of *LMO3* and *HEN2* in aggressive neuroblastomas. As described previously, LMO family protein interacts with the nuclear LIM domain-binding protein 1 and 2 (*Ldb1* and *Ldb2*), which act as adaptors for several LIM domain-containing proteins (30–32), and also binds to the basic helix-loop-helix transcription factor, *TAL1*, to regulate its transcriptional activity (12, 33, 34). Of interest, *HEN1* and *HEN2* were previously identified based on their homology with *TAL1*, and it was shown that *LMO3* was associated with *HEN1* (35). Furthermore, *TAL1* was coexpressed with *LMO1* or *LMO2* in T-cell ALL (36), and double transgenic mice overexpressing *TAL1* and *LMO1* or *LMO2* developed leukemia (37). As shown in Fig. 2A, *LMO3* (A and B) and *HEN2* were expressed at higher levels in unfavorable neuroblastomas compared with favorable tumors, whereas the levels of *LMO1* expression were predominantly high in the favorable tumors. No significant changes in the expression levels of *LMO2*, *Ldb1*, and *Ldb2* were detected between unfavorable and favorable neuroblastomas. *LMO4*, *TAL1*, and *HEN1* showed extremely low levels of expression in both types of neuroblastoma. We then studied the expression of these genes in 10 neuroblastoma and 4 T-cell ALL cell lines to examine the presence or absence of the lineage specificity, neuronal or hematopoietic. Consistent with the previous reports (36), *LMO2* and *TAL1* were coexpressed in T-cell ALL-derived cell lines (RPMI, KOPT, HSB, and MOLT; Fig. 2B). However, of interest, *LMO3* and *Ldb2* were expressed predominantly in neuroblastoma cell lines compared with the leukemia-derived lines. In addition, *HEN2* tended to be less highly expressed in leukemia cells compared with neuroblastoma cells. *HEN1* expression was also restricted to neuroblastoma but limited to only a few cell lines. On the other hand, there was no difference in the expression of *LMO4* and *Ldb1* between neuroblastoma-derived and T-cell ALL-derived cell lines. Interestingly, coexpression of *LMO3* and *HEN2* was observed in the majority of neuroblastoma cell lines but not in the other tumor-derived cell lines with different origin (Fig. 2C). These results revealed that only *LMO3* and *HEN2* were expressed at high levels in aggressive neuroblastomas in a neuronal-specific pattern.

Figure 2D shows the results of *in situ* hybridization for *LMO3* in primary neuroblastomas. *LMO3* mRNA was expressed in a

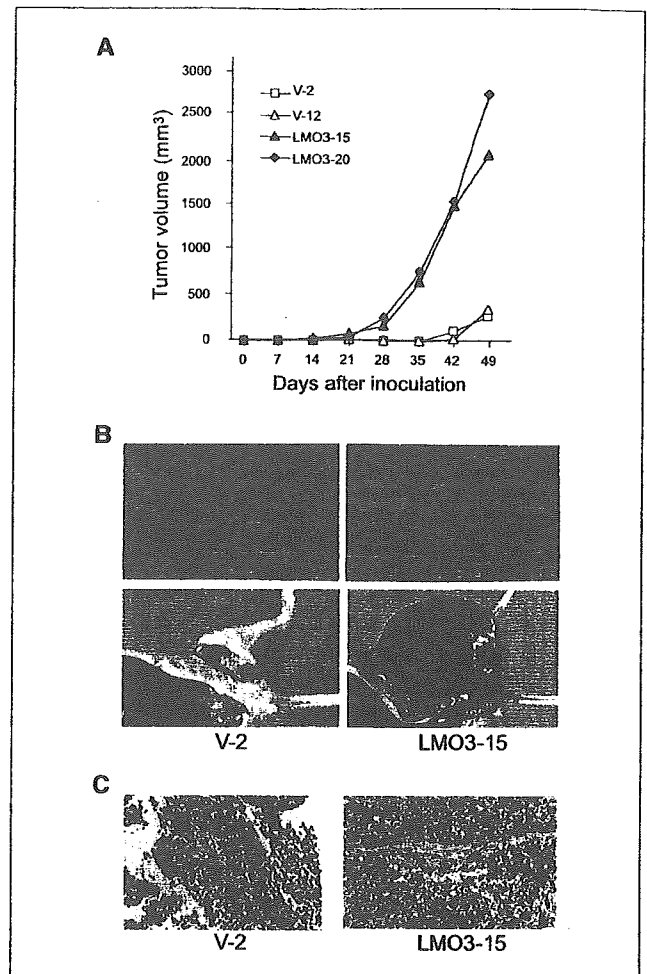


Figure 5. Tumor growth in nude mice. A, nude mice were injected s.c. with 5×10^6 of SH-SY5Y cells or the indicated stable transfectants and tumor volumes were estimated weekly. Points, mean of 8 to 11 independent tumors. B, photographs of the tumors 49 days after s.c. injection of V-2 (left) and LMO3-15 cells (right) into nude mice. C, paraffin sections of the tumors arising from V-2 (left) and LMO3-15 cells (right) were stained with H&E.

stage IV neuroblastoma with *MYCN* amplification, whereas it was negative in a stage I tumor with a single copy of *MYCN* and high expression of *TrkA*. Unfortunately, our antibody raised against human LMO3 protein did not work for the immunohistochemical analysis. The immunostaining of *HEN2* was also strongly positive in the nuclei of most tumor cells in *MYCN*-amplified neuroblastoma, albeit it was negative in favorable subset of the tumor (Fig. 2D).

LMO3 physically interacts with *HEN2*. Because LMO3 and *HEN2* were coexpressed in the majority of unfavorable neuroblastomas as well as neuroblastoma cell lines, we examined whether LMO3 could interact with *HEN2* in mammalian cells. Whole cell lysates prepared from COS7 cells transfected with the expression plasmids for HA-tagged LMO3 and FLAG-tagged *HEN2* were immunoprecipitated with the anti-HA or with the anti-FLAG antibody followed by immunoblotting with the anti-FLAG or with the anti-HA antibody, respectively. As shown in Fig. 3A, FLAG-*HEN2* was coimmunoprecipitated with HA-LMO3. We then examined the subcellular distribution of LMO3 and

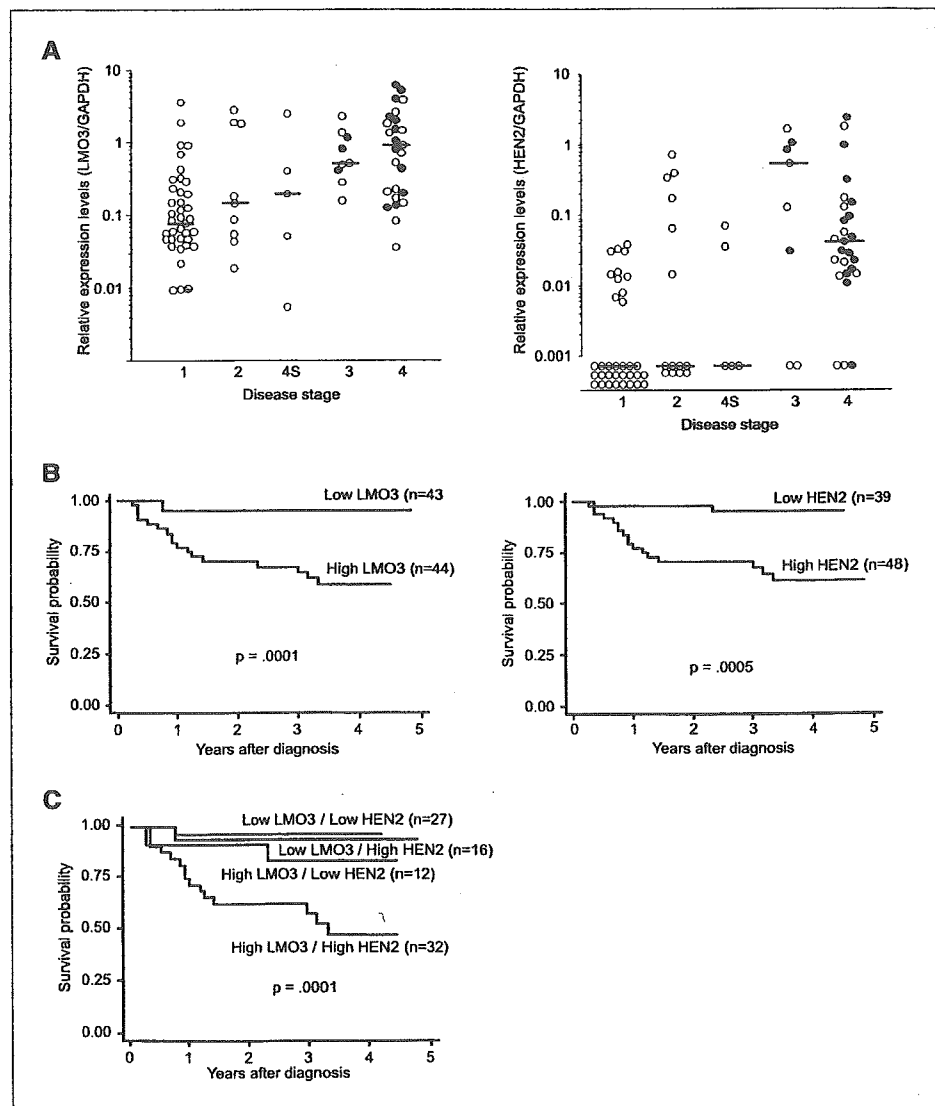
HEN2. COS7 cells were cotransfected with the expression plasmids for HA-LMO3 and FLAG-HEN2 and double stained with anti-HA and anti-FLAG antibodies. As shown in Fig. 3B, LMO3 as well as HEN2 appear exclusively nuclear. On closer inspection by merging two images, these two proteins colocalized in the nucleus. Consistent with the previous reports (35), HA-LMO3 was coimmunoprecipitated with FLAG-HEN1 under our experimental conditions (Fig. 3C).

Overexpression of LMO3 accelerates growth of SH-SY5Y neuroblastoma cells. We addressed the question whether LMO3 could induce cell growth of neuroblastoma. To this end, we transfected the expression plasmid for FLAG-LMO3-A or the empty plasmid into SH-SY5Y neuroblastoma cells and established two stable transfectants overexpressing FLAG-LMO3-A (named as LMO3-15 and LMO3-20). As shown in Fig. 4A, the expression levels of FLAG-LMO3-A were higher in LMO3-15 and LMO3-20 cells than in the parental SH-SY5Y and the control transfectants (V-2 and V-12). LMO3-15 expressed FLAG-LMO3-A at the level comparable with that in LMO3-20. Similar results were also obtained by RT-PCR analysis (Fig. 4B). No obvious morphologic

changes could be observed in LMO3-15 and LMO3-20 cells (data not shown). As shown in Fig. 4C, LMO3-15 and LMO3-20 cells proliferated at a much faster rate than the control transfectants and SH-SY5Y cells in culture medium containing 10% serum. More importantly, LMO3-15 and LMO3-20 cells continued to grow exponentially even in the low serum culture medium, whereas the growth of the vector-transfected cells as well as SH-SY5Y cells was significantly suppressed under this condition.

To examine whether the LMO3-A-overexpressing cells have an ability to grow in soft agar medium, each transfectants were cultured in soft agar medium for 3 weeks. The numbers of colonies with diameters >300 μm formed by each transfectants in soft agar were scored. LMO3-15 and LMO3-20 cells formed large distinct colonies and showed a statistically significant increase in the number of colonies compared with the vector-transfected cells and SH-SY5Y cells (Fig. 4D). These results strongly suggest that overexpression of LMO3 is sufficient to induce malignant transformation in neuroblastoma cells. We also tried to obtain the cells stably transfected with HEN2 but never been successful with unknown reason.

Figure 6. Expression of LMO3 and HEN2 mRNA in 87 primary neuroblastomas. A, expression levels of LMO3 (left) and HEN2 (right) transcripts in 87 primary neuroblastoma samples categorized by the patient's clinical stage were examined by a quantitative real-time RT-PCR. Relative expression levels of LMO3 or HEN2 mRNA were determined by calculating the ratio between GAPDH and LMO3 or HEN2. Bars, median levels of LMO3 or HEN2 expression in each stage; open and closed circles, samples from patients who are alive and dead, respectively. B and C, Kaplan-Meier survival curves of patients with neuroblastomas based on high or low expression of LMO3, HEN2 (B), or LMO3 and HEN2 (C).



LMO3 induces marked tumor growth in nude mice. SH-SY5Y cells with a single copy of *MYCN* form tumors in nude mice, although the growth rate is slow compared with that of the other neuroblastoma cell lines with *MYCN* amplification (38). To examine whether overexpression of LMO3 in SH-SY5Y cells could affect the tumor growth *in vivo*, we injected the each transfectants into the left flank of athymic nude mice, and the tumor volumes were measured weekly. V-2 and V-12 cells slowly formed tumors with similar kinetics and of similar sizes 35 to 42 days after injection (Fig. 5A). In contrast, the tumors grew rapidly in nude mice implanted with LMO3-15 or LMO3-20 cells. The sizes of the excised tumors from the LMO3-15-implanted mice on day 49 were >10-fold larger than those of control mice (Fig. 5B) and showed histologically undifferentiated neuroblastoma with small round cell shapes and small amounts of stromal components (Fig. 5C).

Expression of LMO3 and HEN2 is associated with a poor outcome of neuroblastoma. To verify whether a significant relationship could be observed between the expression of *LMO3* and/or *HEN2* in primary neuroblastomas and the patients' survival, we quantitatively measured the expression levels of *LMO3* and *HEN2* mRNA in 87 primary tumors by using a quantitative real-time RT-PCR. The values of the levels of *LMO3* and *HEN2* expression were normalized to that of *GAPDH* expression [relative expression values (REV)]. The high level of *LMO3* expression was significantly associated with high expression of *HEN2* (Student's *t* tests, mean \pm SE: 1.43 \pm 0.27 REV, *n* = 48 versus 0.54 \pm 0.17 REV, *n* = 39; *P* = 0.001), older age (\geq 1-year-old: 1.37 \pm 0.29, *n* = 32 versus <1-year-old: 0.84 \pm 0.21, *n* = 55; *P* = 0.008), advanced disease stages (stages III + IV: 1.83 \pm 0.35, *n* = 34 versus stages I + II + IVS: 0.52 \pm 0.14; *P* < 0.00005; Fig. 6A), low levels of *TrkA* expression (low *TrkA*: 1.63 \pm 0.34, *n* = 37 versus high *TrkA*: 0.59 \pm 0.15, *n* = 50; *P* = 0.0003), *MYCN* amplification (amplification: 1.91 \pm 0.44, *n* = 27 versus single copy: 0.64 \pm 0.13, *n* = 60; *P* = 0.0002), and sporadic cases of

Table 2. Multiple Cox regression models using LMO3 expression and dichotomous factors of HEN2 expression, age, MYCN amplification, mass screening, and origin (n = 87)

Model	Factor	P	Hazard ratio (95% confidence interval)
A	LMO3 expression (high vs low)	0.005	1.61 (1.16-2.23)
	HEN2 expression (high vs low)	0.029	5.32 (1.19-23.9)
B	LMO3 expression (high vs low)	0.005	1.62 (1.15-2.28)
	Age (>1 vs <1 y)	0.002	5.79 (1.86-18.1)
C	LMO3 expression (high vs low)	0.066	1.36 (0.98-1.89)
	MYCN amplification (1 copy vs >1 copy)	<0.0005	0.075 (.02-.282)
D	LMO3 expression (high vs low)	0.044	1.42 (1.01-2.01)
	Mass screening (+ vs -)	0.005	0.051 (0.007-0.404)
E	LMO3 expression (high vs low)	<0.0005	1.78 (1.31-2.41)
	Origin (adrenal gland vs others)	0.21	2.02 (0.666-6.12)

NOTE: All variables with two categories, except *LMO3* expression (log). Hazard ratio shows the relative risk of death of first category relative to the second.

Table 1. Simple Cox regression models using LMO3 expression and dichotomous factors of HEN2 expression, age, MYCN amplification, mass screening, and origin (n = 87)

Model	Factor	P	Hazard ratio (95% confidence interval)
A	LMO3 expression (high vs low)	<0.0005	1.80 (1.32-2.47)
B	HEN2 expression (high vs low)	0.004	8.69 (2.00-37.7)
C	Age (>1 vs <1 y)	<0.0005	8.75 (2.87-26.7)
D	MYCN amplification (1 copy vs >1 copy)	<0.0005	0.049 (0.014-0.171)
E	Mass screening (+ vs -)	0.001	0.032 (0.004-0.237)
F	Origin (adrenal gland vs others)	0.20	2.06 (0.684-6.23)

NOTE: All variables with two categories, except *LMO3* expression (log). Hazard ratio shows the relative risk of death of first category relative to the second. Because all patients with advanced tumor stages and low expression of *TrkA* had died of the tumor, a Cox regression model with the tumor stage or *TrkA* expression was not fitted.

neuroblastoma (sporadic: 1.68 \pm 0.32, *n* = 39 versus mass screening: 0.51 \pm 0.14, *n* = 48; *P* < 0.00005). The high level of *HEN2* expression was also significantly correlated with high expression of *LMO3* (χ^2 tests: *P* = 0.001), older age (*P* < 0.0005), advanced stages (*P* < 0.0005; Fig. 6B), low *TrkA* expression (*P* < 0.0005), *MYCN* amplification (*P* < 0.0005), and sporadic cases of neuroblastoma (*P* < 0.0005). Thus, high expression of *LMO3* and *HEN2* was well associated with conventional markers indicating the poor prognosis of neuroblastoma.

We next tested if expression levels of *LMO3* and *HEN2* could have prognostic significance in primary neuroblastomas. The results for log-rank tests showed that high expression of *LMO3* or *HEN2* was significantly associated with poor survival (*P* = 0.0002 and 0.0005, respectively; Fig. 6C and D). Remarkably, the combination of high expression of both *LMO3* and *HEN2* showed the significantly worse prognosis compared with the other combinations of *LMO3* and *HEN2* expression levels as shown in Fig. 6E. As expected, older patients and the patients with advanced tumors, low expression of *TrkA*, amplified *MYCN*, and the tumors found by mass screening were associated with short time to survival (*P* < 0.00005). However, the adrenal origin of the tumor was not associated with the outcome (*P* = 0.19; data not shown).

The univariate analysis suggested that *LMO3* expression (*P* < 0.0005), *HEN2* expression (*P* = 0.004), age (*P* < 0.0005), *MYCN* amplification (*P* < 0.0005), and mass screening (*P* = 0.001) were of prognostic importance, supporting the results of the log-rank test (Table 1). Furthermore, the multivariate analysis showed that

LMO3 expression was significantly associated with survival after controlling HEN2 expression ($P = 0.005$), age ($P = 0.005$), mass screening ($P = 0.044$), and origin ($P < 0.0005$), suggesting that LMO3 expression was an independent prognostic factor from the other factors (Table 2). LMO3 expression was marginally associated with survival after controlling MYCN amplification ($P = 0.066$). On the other hand, because HEN2 expression was highly associated with age, MYCN amplification, and mass screening, it was not significantly associated with survival after controlling age, MYCN amplification, and mass screening in the corresponding multiple Cox regression models (data not shown).

Discussion

In the present study, we have identified that both LMO3 and HEN2 are expressed at higher levels in aggressive neuroblastomas especially with MYCN amplification than those with favorable prognosis. Coexpression of LMO3 and HEN2 has been observed almost exclusively in neuroblastoma cell lines, not the other lines, suggesting that their expression and function are neuronal specific. Furthermore, LMO3 physically interacted with HEN2 in mammalian cells. The functional significance of LMO3 expression was shown by a stable transfection into SH-SY5Y neuroblastoma cells, colony formation in soft agar, and tumor growth in nude mice, all of which have suggested that LMO3, probably by interacting with endogenous HEN2, markedly promotes the tumor growth. Indeed, the tumors with high expression of both LMO3 and HEN2 have shown the worst prognosis in the analysis of 87 primary neuroblastomas. Thus, our results suggested that, in concert with HEN2, the neuronal specifically expressed LMO3 plays an important role in the tumorigenesis of neuroblastoma. Our observation is strikingly intriguing because that LMO1 or LMO2 is already known to be the oncogene in T-cell acute lymphoblastic leukemia and that LMO4 has recently been implicated in the genesis of breast cancer (4, 9).

We have identified a *Nbla3267/LMO3* clone from the screening of differentially expressed genes between favorable and unfavorable subsets of neuroblastoma. LMO3 was one of the genes expressed at higher levels in the latter than the former (24), like MYCN oncogene and DDX1, a DEAD box gene coamplified with MYCN in aggressive neuroblastomas. In the development of hematopoietic system, LMO1 and LMO2 form a transcriptional complex with Ldb1, a LIM domain-binding protein, and a basic helix-loop-helix protein TAL1, which was identified as an oncogene at the translocation breakpoint in T-cell ALL (4-7). From the analogy with the LMO1 or LMO2 transcriptional machinery in T-cell ALL, we searched for the similar complex in the neuronal system by using the different subsets of primary neuroblastoma and the cell lines in comparison with the T-cell ALL cell lines. As a result, the neuronal-specific pattern of expression was observed in LMO3, Ldb2, HEN1, and HEN2, among which LMO3 and HEN2 were significantly highly expressed in the unfavorable subset of neuroblastomas with MYCN amplification compared with the favorable subset. This result strongly suggested that LMO3 may function in collaboration with HEN2 in advanced stages of neuroblastoma. Indeed, both genes were coexpressed only in neuroblastoma derived-cell lines, not in other tumor-derived ones, suggesting that their expression is lineage specific. Furthermore, LMO3 and HEN2

physically interacted in mammalian cells, albeit with weak interaction between LMO3 and HEN1 (35). Thus, these results also suggest that LMO3 and HEN2 form a neuronal cassette mimicking the hematopoietic complex composed of LMO2 and TAL1 and regulate the growth of neuroblastoma.

The neuronal-specific basic helix-loop-helix transcription factors, HEN1 and HEN2, were originally identified from the cDNA library of a neuroblastoma cell line based on cross-hybridization with TAL1 (14, 15). Their expression was restricted to the developing nervous system and a neuroblastoma cell line. However, their function has long been unclear. Recently, Bao et al. have reported that HEN1 interacts with LMO proteins by yeast two-hybrid screen and that *Xenopus* HEN1, in concert with XLMO3, is a critical regulator of neurogenesis (35). This prompted us to test our hypothesis both *in vitro* and *in vivo*. As the results, we found that the SH-SY5Y neuroblastoma cells stably overexpressing LMO3, presumably by acting with endogenous HEN2, gained rapid cell growth in the culture medium with 10% or 1% serum, in the soft agar medium, and in nude mice. These suggested that LMO3 is a neuronal-specific oncogene in neuroblastoma, without any rearrangement of the LMO3 gene (data not shown). However, we failed to establish a stable SH-SY5Y cell line transfected with HEN2. It is presumed that overexpression of HEN2 might have caused cell death or growth arrest in the cells, albeit the reason is elusive.

The double transgenic mice overexpressing LMO2 and TAL1 displayed a more rapid development of leukemia compared with those overexpressing LMO2 alone, suggesting that LMO2 and TAL1 act synergistically through their complex formation in the development of leukemia (13). Of note, Ono et al. reported that LMO2 and TAL1 act as cofactors for GATA3 to induce the expression of the *retinaldehyde dehydrogenase 2* gene in T-cell ALL (39). On the other hand, a stable complex comprising LMO2, TAL1, and GATA1 was required to promote erythroid differentiation (32). Therefore, LMO3 and HEN2 may also form a nuclear complex, including family members of GATA to regulate cell growth and differentiation in neuroblastoma. Our preliminary data have suggested that GATA2, GATA3, GATA4, and GATA6 are highly expressed in neuroblastoma cell lines, among which GATA4 and GATA6 are predominantly coexpressed in neuroblastoma cell lines compared with T-cell ALL lines. Thus, LMO3 and HEN2, in collaboration with GATA and Ldb families, may play a role in determining cell fate in both neural development and neuroblastoma genesis, although this hypothesis needs to be elucidated. Recently, it has been shown that LMO3 enhanced the ability of HEN1 through the physical interaction to transactivate the expression of *Neurogenin-1* as well as *NeuroD* and thereby induced the neuronal differentiation in frog embryos (35). We tested if this is the case in the neuroblastoma cells. However, our preliminary results suggested that the LMO3/HEN2 complex does not transactivate the *Neurogenin-1* as well as *NeuroD* promoter in neuroblastoma cell lines,⁵ although it is unclear if the complex could work in normal neuronal development. Thus, like LMO2, alterations in the LMO3-containing transcriptional complex might differentially regulate expression of the downstream target genes closely involved in neuronal differentiation or tumor formation.

⁵ Unpublished data.

It is striking that high levels of expression of both *LMO3* and *HEN2* are significantly associated with the poor prognosis in primary neuroblastomas. This clearly reflects how importantly both genes are functioning in the progression of neuroblastoma *in vivo*. Of interest, expression of either gene is well correlated with *MYCN* amplification, raising the possibility that they might be the downstream targets of *MYCN*. However, we could not confirm it in human neuroblastoma cell line SH-EP in which *MYCN* was regulated under the control of the rTet-inducible expression system (40). In agreement with this, cDNA microarray-based screening for the genes induced in the *MYCN*-amplified neuroblastoma cells thus far failed to detect either *LMO3* or *HEN2* (41, 42). The link between *LMO* family molecules and the other oncogenes or tumor suppressor genes is also important. Despite the lack of prognostic significance, *LMO4* overexpressed in breast cancer seems to be indispensable in the mammary carcinogenesis because it interacts with both *BRCA1* and *CtIP* to repress the *BRCA1* function (10). This suggests that, similarly to *LMO4*, *LMO3* may also have the interacting partners related to the tumorigenesis. Thus, *LMO3* and *HEN2* as well as their associated molecules might be good candidates for the future targets of the therapy against aggressive neuroblastomas.

Acknowledgments

Received 12/28/2004; revised 3/9/2005; accepted 3/23/2005.

Grant support: Grant-in-Aid from the Ministry of Health, Labour and Welfare for Third Term Comprehensive Control Research for Cancer, Grant-in-Aid for Scientific Research on Priority Areas from the Ministry of Education, Culture, Sports, Science and Technology, Japan, and Grant-in-Aid for Scientific Research from Japan Society for the Promotion of Science. M. Aoyama is an awardee of the Research Resident Fellowship from the Foundation for Promotion of Cancer Research in Japan.

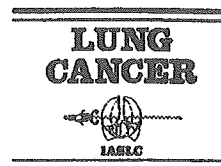
The costs of publication of this article were defrayed in part by the payment of page charges. This article must therefore be hereby marked *advertisement* in accordance with 18 U.S.C. Section 1734 solely to indicate this fact.

We thank S. Sakiyama for critical reading of the article; A. Morohashi, N. Kitabayashi, H. Murakami, and N. Sugimitsu for excellent technical assistance; and the following institutions and hospitals for supplying the tumor samples: Department of Pediatric Surgery, Iwaki Kyoritsu Hospital; Departments of Pediatrics and Pediatric Surgery, Aichi Medical University; Department of Pediatrics, Nara Hospital; Department of Pediatrics, Kyoto Prefectural University of Medicine; Department of Pediatric Surgery, Kimitsu Central Hospital; Department of Surgery, Gunma Children's Medical Center; Department of Pediatrics, Sapporo National Hospital; Departments of Pediatrics, Pediatric Surgery, and General Surgery, Jichi Medical School; Departments of Pediatrics and Pediatric Surgery, Kagoshima University; Department of Pediatrics, Juntendo University; Department of Pediatric Surgery, Showa University; Department of Pediatric Surgery, Niigata University; Departments of Surgery and Pathology, Chiba Children's Hospital; Department of Pediatric Surgery, Chiba University; Department of Pediatric Surgery, Osaka City General Hospital; Department of Pediatric Surgery, Tsukuba University; Department of Pediatric Surgery, Tokai University; Department of Surgery, Tokyo Metropolitan Kiyose Children's Hospital; Department of Pediatric Surgery, Tohoku University; Tomor Board, Hyogo Prefectural Kobe Children's Hospital; and First Department of Surgery, Hokkaido University.

References

- Dawid IB, Breen JJ, Toyama R. LIM domains: multiple roles as adaptors and functional modifiers in protein interactions. *Trends Genet* 1998;14:156-62.
- Sanchez-Garcia I, Rabbitts TH. The LIM domain: a new structural motif found in zinc-finger-like proteins. *Trends Genet* 1994;10:315-20.
- Dawid IB, Toyama R, Taira M. LIM domain proteins. *C R Acad Sci III* 1995;318:295-306.
- Rabbitts TH. *LMO* T-cell translocation oncogenes typify genes activated by chromosomal translocations that alter transcription and developmental processes. *Genes Dev* 1998;12:2651-7.
- McGuire EA, Rintoul CE, Sclar GM, Korsmeyer SJ. Thymic overexpression of Ttg-1 in transgenic mice results in T-cell acute lymphoblastic leukemia/lymphoma. *Mol Cell Biol* 1992;12:4186-96.
- Fisch P, Boehm T, Lavenir I, et al. T-cell acute lymphoblastic lymphoma induced in transgenic mice by the *RBTN1* and *RBTN2* LIM-domain genes. *Oncogene* 1992;7:2389-97.
- Neale GA, Reh JE, Goorha RM. Disruption of T-cell differentiation precedes T-cell tumor formation in *LMO-2* (rhombotin-2) transgenic mice. *Leukemia* 1997;3:289-90.
- Kenny DA, Jurata LW, Saga Y, Gill GN. Identification and characterization of *LMO4*, an *LMO* gene with a novel pattern of expression during embryogenesis. *Proc Natl Acad Sci U S A* 1998;95:11257-62.
- Visvader JE, Venter D, Hahn K, et al. The LIM domain gene *LMO4* inhibits differentiation of mammary epithelial cells *in vitro* and is overexpressed in breast cancer. *Proc Natl Acad Sci U S A* 2001;98:14452-7.
- Sum EY, Peng B, Yu X, et al. The LIM domain protein *LMO4* interacts with the cofactor *CtIP* and the tumor suppressor *BRCA1* and inhibits *BRCA1* activity. *J Biol Chem* 2002;277:7849-56.
- Feroni L, Boehm T, White L, et al. The rhombotin gene family encode related LIM-domain proteins whose differing expression suggests multiple roles in mouse development. *J Mol Biol* 1992;226:747-61.
- Wadman I, Li J, Bash RO, et al. Specific *in vivo* association between the bHLH and LIM proteins implicated in human T cell leukemia. *EMBO J* 1994;13:4831-9.
- Larson RC, Lavenir I, Larson TA, et al. Protein dimerization between *Lmo2* (*Rbtn2*) and *Tal1* alters thymocyte development and potentiates T cell tumorigenesis in transgenic mice. *EMBO J* 1996;15:1021-7.
- Brown L, Espinosa R III, Le Beau MM, Siciliano MJ, Baer R. *HEN1* and *HEN2*: a subgroup of basic helix-loop-helix genes that are coexpressed in a human neuroblastoma. *Proc Natl Acad Sci U S A* 1992;89:8492-6.
- Begley CG, Lipkowitz S, Gobel V, et al. Molecular characterization of *NSCL*, a gene encoding a helix-loop-helix protein expressed in the developing nervous system. *Proc Natl Acad Sci U S A* 1992;89:38-42.
- Brodeur GM, Azar C, Brother M, et al. Effect of genetic factors on prognosis and treatment. *Cancer* 1992;70:1685-94.
- Brodeur GM, Nakagawara A. Molecular basis of clinical heterogeneity in neuroblastoma. *J Pediatr Hematol Oncol* 1992;14:111-6.
- Brodeur GM, Seeger RC, Schwab M, Varmus HE, Bishop JM. Amplification of *N-myc* in untreated human neuroblastomas correlates with advanced disease stage. *Science* 1984;224:1121-4.
- Seeger RC, Brodeur GM, Sather H, et al. Association of multiple copies of the *N-myc* oncogene with rapid progression of neuroblastomas. *N Engl J Med* 1985;313:1111-6.
- Nakagawara A, Arima M, Azar CG, Scavarda NJ, Brodeur GM. Inverse relationship between *trk* expression and *N-myc* amplification in human neuroblastomas. *Cancer Res* 1992;52:1364-8.
- Nakagawara A, Arima-Nakagawara M, Scavarda NJ, Azar CG, Cantor AB, Brodeur GM. Association between high levels of expression of the *TRK* gene and favorable outcome in human neuroblastoma. *N Engl J Med* 1993;328:847-54.
- Gross N, Beretta C, Peruisseau G, Jackson D, Simmons D, Beck D. CD44H expression by human neuroblastoma cells: relation to *MYCN* amplification and lineage differentiation. *Cancer Res* 1994;54:4238-42.
- Berwanger B, Hartmann O, Bergmann E, et al. Loss of a FYN-regulated differentiation and growth arrest pathway in advanced stage neuroblastoma. *Cancer Cell* 2002;2:377-86.
- Ohira M, Morohashi A, Inuzuka H, et al. Expression profiling and characterization of 4200 genes cloned from primary neuroblastomas: identification of 305 genes differentially expressed between favorable and unfavorable subsets. *Oncogene* 2003;22:5525-36.
- Ohira M, Shishikura T, Kawamoto T, et al. Hunting the subset-specific genes of neuroblastoma: expression profiling and differential screening of the full-length-enriched oligo-capping cDNA libraries. *Med Pediatr Oncol* 2000;35:547-9.
- Brodeur GM, Pritchard J, Berthold F, et al. Revisions of the international criteria for neuroblastoma diagnosis, staging, and response to treatment. *J Clin Oncol* 1993;11:1466-77.
- Matsumura T, Iehara T, Sawada T, Tsuchida Y. Prospective study for establishing the optimal therapy of infantile neuroblastoma in Japan. *Med Pediatr Oncol* 1998;31:210.
- Kaneko M, Nishihira H, Mugishima H, et al. Study Group of Japan for Treatment of Advanced Neuroblastoma, Tokyo, Japan. Stratification of treatment of stage 4 neuroblastoma patients based on *N-myc* amplification status. *Med Pediatr Oncol* 1998;31:1-7.
- Takahara Y, Tomotsune D, Shirai M, et al. Targeted disruption of the mouse homologue of the *Drosophila* polyhomeotic gene leads to altered anteroposterior patterning and neural crest defects. *Development* 1997;124:3673-82.
- Agulnick AD, Taira M, Breen JJ, Tanaka T, Dawid IB, Westphal H. Interactions of the LIM-domain-binding factor *Ldb1* with LIM homeodomain proteins. *Nature* 1996;384:270-2.
- Jurata LW, Kenny DA, Gill GN. Nuclear LIM interactor, a rhombotin and LIM homeodomain interacting protein, is expressed early in neuronal development. *Proc Natl Acad Sci U S A* 1996;93:11693-8.
- Bach I, Carriere C, Ostendorff HP, Andersen B, Rosenfeld MG. A family of LIM domain-associated cofactors confer transcriptional synergism between LIM and Otx homeodomain proteins. *Genes Dev* 1997;11:1370-80.
- Osada H, Grutz G, Axelson H, Forster A, Rabbitts TH. Association of erythroid transcription factors: complexes involving the LIM protein *RBTN2* and the zinc-finger protein *GATA1*. *Proc Natl Acad Sci U S A* 1995;92:9585-9.
- Valge-Archer VE, Osada H, Warren AJ, et al. The LIM protein *RBTN2* and the basic helix-loop-helix protein *TAL1* are present in a complex in erythroid cells. *Proc Natl Acad Sci U S A* 1994;91:8617-21.
- Bao J, Talmage DA, Role LW, Gautier J. Regulation of neurogenesis by interactions between *HEN1* and neuronal *LMO* proteins. *Development* 2000;127:425-35.

36. Ono Y, Fukuhara N, Yoshie O. Transcriptional activity of TAL1 in T cell acute lymphoblastic leukemia (T-ALL) requires RBTN1 or -2 and induces TALLA1, a highly specific tumor marker of T-ALL. *J Biol Chem* 1997;272:4576-81.
37. Aplan PD, Jones CA, Chervinsky DS, et al. An scl gene product lacking the transactivation domain induces bony abnormalities and cooperates with to generate T-cell malignancies in transgenic mice. *EMBO J* 1997;16:2408-19.
38. Eggert A, Grotzer MA, Ikegaki N, Liu XG, Evans AE, Brodeur GM. Expression of the neurotrophin receptor TrkA down-regulates expression and function of angiogenic stimulators in SH-SY5Y neuroblastoma cells. *Cancer Res* 2002;62:1802-8.
39. Ono Y, Fukuhara N, Yoshie O. TAL1 and LIM-only proteins synergistically induce retinaldehyde dehydrogenase 2 expression in T-cell acute lymphoblastic leukemia by acting as cofactors for GATA3. *Mol Cell Biol* 1998;18:6939-50.
40. Lutz W, Stohr M, Schurmann J, Wenzel A, Lohr A, Schwab M. Conditional expression of *N-myc* in human neuroblastoma cells increases expression of α -prothymosin and ornithine decarboxylase and accelerates progression into S-phase early after mitogenic stimulation of quiescent cells. *Oncogene* 1996;13:803-12.
41. Schuldiner O, Benvenisty N. A DNA microarray screen for genes involved in c-MYC and N-MYC oncogenesis in human tumors. *Oncogene* 2001;20:4984-94.
42. Shohet JM, Hicks MJ, Plon SE, et al. Minichromosome maintenance protein MCM7 is a direct target of the MYCN transcription factor in neuroblastoma. *Cancer Res* 2002;62:1123-8.



Aberrant methylation of *FBN2* in human non-small cell lung cancer

Hong Chen^{a,c}, Makoto Suzuki^{a,d,*}, Yohko Nakamura^b, Miki Ohira^b,
Soichiro Ando^a, Tomohiko Iida^{a,d}, Takahiro Nakajima^{a,d},
Akira Nakagawara^b, Hideki Kimura^a

^a Division of Thoracic Diseases, Chiba Cancer Center, 666-2, Nitona, Chuoh-ku, Chiba 260-8717, Japan

^b Division of Biochemistry, Chiba Cancer Center, 666-2, Nitona, Chuoh-ku, Chiba 260-8717, Japan

^c Department of Pulmonary Disease, The First Affiliated Hospital, Chongqing Medical University, 1 Youyi Road, Yuzhong District, Chongqing 400016, China

^d Department of Thoracic Surgery, Graduate School of Medicine, Chiba University, 1-8-1 Inohana, Chuoh-ku, Chiba 260-8670, Japan

Received 27 December 2004; received in revised form 5 April 2005; accepted 12 April 2005

KEYWORDS

FBN2;
Methylation;
Lung cancer;
Invasion;
Metastasis

Summary *FBN2*, a large modular extracellular matrix glycoprotein, is known to be a key component of human elastic fiber. A loss of *FBN2* expression due to promoter methylation was recently identified in pancreatic cancer. We examined *FBN2* expression by reverse transcription PCR and aberrant methylation of *FBN2* by methylation specific PCR in lung cancer cell lines. Aberrant methylation of *FBN2* was present in 55% (6 of 11) of non-small cell lung cancer (NSCLC) cell lines, but it absent in small cell lung cancer cell lines. The concordance between loss of expression and aberrant methylation of *FBN2* was 88% (14 of 16) in the cell lines. *FBN2* expression was restored after treatment with the demethylating agent, 5-aza-2'-deoxycytidine in all six cell lines tested that lacked *FBN2* expression. Among primary NSCLC, 49% (62/126) of cases had *FBN2* methylation, but only 7% (5/69) of the corresponding nonmalignant lung tissues had it. Although *FBN2* methylation was detected even in patients with early stage disease, it occurred frequently in large tumors ($p=0.022$), with nodal metastasis ($p=0.037$), or with advanced stages of NSCLC ($p=0.014$). Methylation and silencing of *FBN2* in tumor cells may play an important role in carcinogenesis, invasion, and metastasis of NSCLC.

© 2005 Elsevier Ireland Ltd. All rights reserved.

1. Introduction

It is well known that genetic abnormalities of proto-oncogenes and tumor suppressor genes (TSGs) are frequently involved in lung cancer pathogenesis.

* Corresponding author. Tel.: +81 43 222 7171x5464;
fax: +81 43 226 2172.

E-mail address: suzumako@ra2.so-net.ne.jp (M. Suzuki).

The mechanism for inactivation of TSGs is gradually becoming more clearly understood. Epigenetic inactivation of certain TSGs by aberrant promoter methylation is frequently observed in lung cancer and seems to play an important role in the pathogenesis of this cancer [1–4]. In addition, the study of the loss of heterozyosity (LOH) which is also involved in the carcinogenesis of lung cancer, showed that correlations between LOH on different chromosomes suggested previously unknown genetic interactions for lung cancer development [5]. So, whereas the DNA methylation of multiple genes has been studied in lung cancer [6–8], further studies of epigenetic alternation are still needed to clarify fully the biological mechanism of lung cancer.

Fibrillin 2 (FBN2), an extracellular matrix protein, is associated with elastic fibers in several tissues and is believed to serve as a ligand for α v β 3 integrin, the latter being a known morphogen. FBN2 was first expressed in the mesenchyme and at the epitheliomesenchymal interface. Later, its expression was intensified and was confined around the tracheobronchial airways. Fibrillin-2 antisense oligodeoxynucleotide can induce dysmorphogenesis of the lung explants. FBN2 plays a key role in lung development [9].

Recently, the loss of FBN2 expression due to promoter methylation was identified in pancreatic cancer cell lines by means of high-throughput microarray analysis [10]. Of the 12 genes silenced by methylation of 5' regions, FBN2 was methylated in about 75% of the samples, which is a much higher proportion than for the other genes. This gene maps to 5q23-q31, a locus frequently showing allelic imbalance in lung cancer, and was speculated to act as a TSG [5]. This prompted us to examine the methylation status of FBN2 in lung cancers. We examined methylation by methylation specific PCR (MSP), and the mRNA expression of FBN2 by reverse transcription PCR (RT-PCR), in lung cancer cell lines, and analyzed the methylation status of primary lung cancers, and then correlated this with the clinico-pathological features.

2. Materials and methods

2.1. Cell lines and clinic samples

Eleven non-small cell lung cancer (NSCLC) and five small cell lung cancer (SCLC) cell lines were used in this study. These cell lines were established and provided by Dr. Adi F. Gazdar of University of Texas

(UT) Southwestern Medical Center. Cell lines having the prefix NCI were established at the National Cancer Institute, while those with the prefix HCC were established at UT Southwestern Medical Center. They were grown in RPMI-1640 medium supplemented with 5% fetal bovine serum and incubated in 5% CO₂ at 37°C. Nonmalignant human bronchial epithelial cells (NHBE) were cultured as reported previously [11], and normal tracheal RNA was obtained from Clontech (Palo Alto, CA).

Surgically resected specimens of 126 patients with primary lung cancer and 69 adjacent lung tissues were obtained from Chiba Cancer Center, Japan, after obtaining Institutional Review Board approval and informed consent had been granted. Samples were immediately frozen and stored at –80°C until used. The clinical characteristics of these patients are detailed in Table 1.

2.2. RNA preparation and RT-PCR

FBN2 mRNA expression was examined by RT-PCR. Total RNA was obtained from these cell lines (NHBE, 11 NSCLC and 5 SCLC cell lines) by the single-step method. The reverse transcription reaction was performed on 5 µg of total RNA with the SuperScript II First-Strand Synthesis using oligo(dT) primer System (Life Technologies Inc.), and aliquots of the reaction mixture were used for the subsequent PCR amplification. Expression of β -actin was used as an internal control to confirm the success of the reverse transcription reaction. The forward PCR amplification primer of FBN2 was 5'-GGCGAGGACAGCAGGAC-3', and the reverse primer 5'-TGATATTTGCCCACTGGAACA-3'. The forward PCR amplification primer of β -actin was 5'-CAACTGGGACGACATGGAGA-3', and the reverse primer 5'-ACGTACATGGTGGGGTGTG-3'. These primer sequences were identical to the human target genes as was confirmed by BLAST searches. PCR products were analyzed on 2% agarose gels stained with ethidium bromide. NHBE and normal tracheal cells were used as normal controls for RT-PCR.

2.3. 5-Aza-2'-deoxycytidine (5-Aza-CdR) treatment

Six tumor cell lines with negative gene expression were incubated in culture medium with 1 µM of the demethylating agent 5-aza-dC (Sigma-Aldrich, St. Louis, Mo) for 6 days, with medium changes on days one, three and five. Cells were harvested and RNA was extracted at day 6.

Table 1 Clinical characteristics and *FBN2* methylation of lung cancer patients

Clinical factors	No. of cases	No. of <i>FBN2</i> methylation (%)	<i>p</i> -value ^a
Gender			
Male	73	38 (52)	NS
Female	53	24 (45)	
Age			
≤65 ^b	58	25 (43)	NS
>65	68	37 (54)	
Smoke			
Never	47	20 (43)	NS
Smoker	79	42 (53)	
Histology			
Adenocarcinoma	92	49 (53)	NS ^c
Squamous cell carcinoma	30	11 (37)	
Others (ad-sq, Large)	4	2 (50)	
pT			
T1	53	20 (38)	0.022
T2, 3, 4	73	42 (58)	
pN			
N0	76	32 (42)	0.037
N1, 2, 3	50	30 (60)	
pStage			
I	54	20 (37)	0.014
II, III, IV	72	42 (58)	

^a Fisher's exact probability test.

^b Divided into two groups by median age.

^c Adenocarcinoma vs. squamous cell carcinoma ad-sq, adeno-squamous cell carcinoma; NS, not significant.

2.4. DNA preparation, bisulfite modification and MSP

Genomic DNA was obtained from lung cancer cell lines, cultured nonmalignant cells, primary tumors and adjacent nonmalignant tissues by digestion with proteinase K (Life Technologies, Inc.), followed by phenol/chloroform (1:1) extraction [12]. One microgram of genomic DNA was further subjected to bisulfite treatment following the protocol of the EZ DNA Methylation Kit (Zymo Research). The modified DNA was used as a template for MSP. DNA methylation patterns in the CpG island of *FBN2* were determined by the method of MSP as reported previously [10]. Primer sequences of *FBN2* for the unmethylated reaction were: 5'-TATGGGAAT -TTGTTGAGTTTTGT-3' (sense), and 5'-AACCAACAACCCCAAACA-3' (antisense), which amplify a 171 bp product. Primer sequences of *FBN2* for the methylated reaction were: 5'-GGGAATTCGTCGAGTTTTGC-3' (sense), and 5'-AACCGACAACCCCGAACG-3' (antisense),

which amplify a 168 bp product. Universal Methylated DNA (Chemicon, CA) which was subjected to bisulfite treatment was used as a positive control for methylated alleles. Controls without DNA were included in each assay. Nine microlitre of each PCR product was loaded on 2% agarose gels stained with ethidium bromide. Results were confirmed by repeating the bisulfite treatment and MSP for all samples.

2.5. Statistical analysis

The differences of methylation between the two groups were analyzed by using Fisher's exact test. Survival was calculated from the date of initial diagnosis until death or the date of the last follow-up. Survival was analyzed, according to the Kaplan-Meier method, and differences in their distribution were evaluated by means of the log-rank test. A probability value of *p* less than 0.05 was regarded as statistically significant. All *P*s are two-sided.

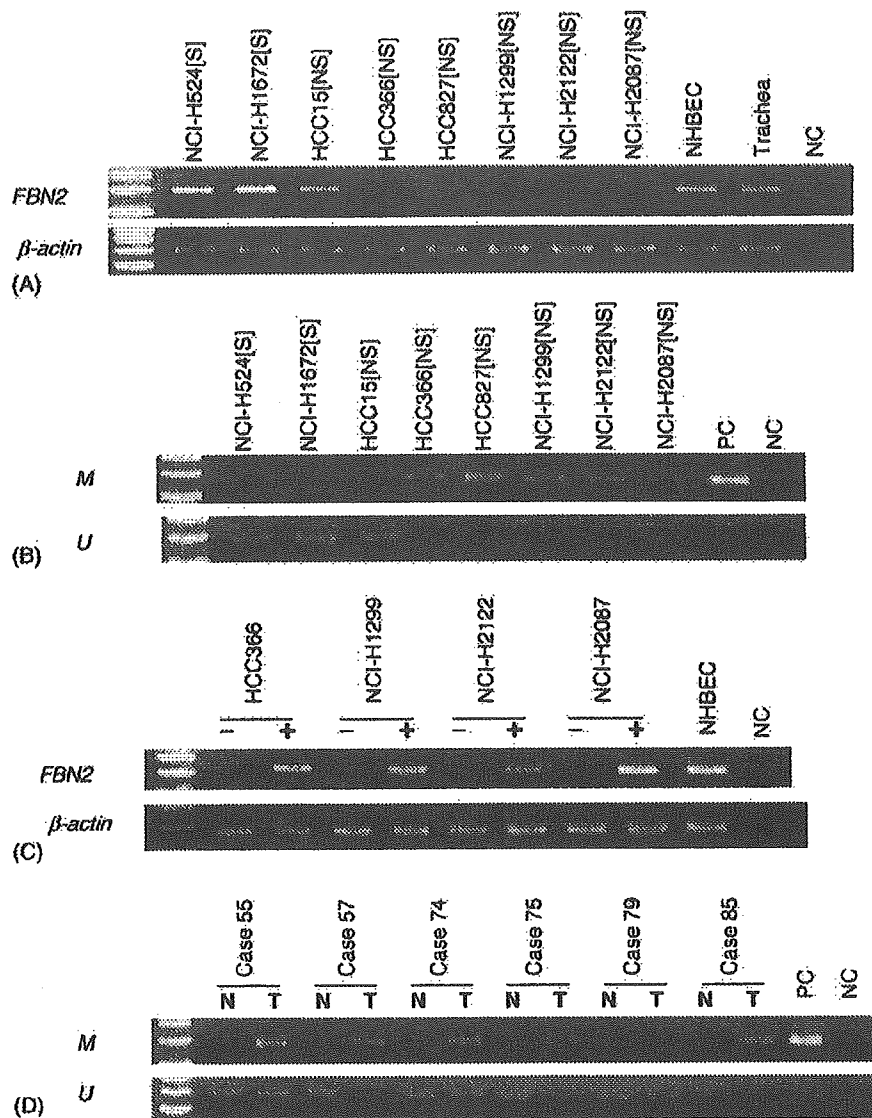


Fig. 1 (A) Representative examples of RT-PCR assay for *FBN2* RNA expression in NSCLC and SCLC cell lines. Expression of β -actin was used as a control for cDNA normalization. NHBEC and trachea were used as positive controls; NC, negative control. [NS], NSCLC; [S], SCLC. Lanes that do not show a band represent samples with loss of expression. (B) Methylation analysis of *FBN2* in cell lines. Lane U, amplified product with primers recognizing an unmethylated sequence (171-bp PCR product); Lane M, amplified product with primers recognizing a methylated sequence (168-bp PCR product). PC, positive control; NC, negative control. C, reexpression of *FBN2* after treatment with 5-Aza-2'-deoxycytidine (5-Aza-CdR). The expression of *FBN2* lost in those cell lines can be restored after treatment with 5-Aza-CdR. -, cell line without 5-Aza-CdR; +, cell line with 5-Aza-CdR; NHBEC was used as the positive control. (D), Representative examples of methylation analysis of *FBN2* in tumor specimens. N, nonmalignant lung tissue; T, tumor.

3. Results

3.1. Expression of *FBN2* in cell lines

FBN2 expression was examined by RT-PCR, and representative examples are shown in Fig. 1. Expression of *FBN2* was present in NHBEC and normal trachea. However, loss of *FBN2* expression was observed in 50% (8/16) of lung cancer cell

lines, respectively, in 64% (7/11) of NSCLC cell lines, and in 20% (1/5) of SCLC cell lines.

3.2. Aberrant methylation of *FBN2* in cell lines

Detailed results of the aberrant methylation of *FBN2* in cell lines are shown in Fig. 1. Aberrant methylation was absent in NHBEC, but was observed

in 38% (6/16) of lung cancer cell lines, in 55% (6/11) of NSCLC cell lines, but in no SCLC cell lines. Only two cell lines (NCI-H524 and HCC15) demonstrated loss of expression and lack of methylation of *FBN2*. The concordance between gene expression and methylation of *FBN2* was 91% (10/11) in the NSCLC cell lines, and 80% (4/5) in the SCLC cell lines (overall concordance: 88%).

3.3. 5-Aza-CdR treatment

To confirm that the promoter methylation was responsible for silencing the *FBN2* expression, we treated methylated NSCLC cell lines (HCC366, HCC827, NCI-H1299, NCI-H2087, NCI-H2122, and NCI-H2887) that showed loss of *FBN2* expression with the demethylating agent 5-Aza-CdR. *FBN2* expression was restored after the treatment in all six cell lines tested (Fig. 1).

3.4. Aberrant methylation of *FBN2* in primary lung cancers

FBN2 methylation of primary tumors and corresponding nonmalignant tissues are detailed in Table 1 and representative samples are illustrated in Fig. 1. *FBN2* methylation was observed in 49% (62/126) of tumors, but in only 7% (5/69) of corresponding nonmalignant tissues. Methylation was tumor-specific when compared with that of corresponding nonmalignant lung tissue ($p < 0.0001$).

FBN2 methylation with clinico-pathological features was also examined. There were no significant correlations in gender, age, smoking history (ever versus never smoked). The aberrant methylation of *FBN2* gene was present in 53% (49/92) cases of adenocarcinoma, and in 37% (11/30) of the squamous cell carcinoma cases. The difference between these results is not significant ($p = 0.09$). Because the number of squamous cell carcinomas and other histologies was small, we carried out a further study on the whole population of patients, unclassified by histology. The frequency of *FBN2* methylation was higher in the later T stages (T2, 3, 4) than in T1 ($p = 0.022$), higher in the later N stages (N1, 2, 3) than in N0 ($p = 0.037$), and in the later stages (II, III, IV) than in stage I ($p = 0.014$). However, *FBN2* methylation status did not correlate with survival ($p = 0.37$, log-rank test). The Cox proportional hazards model was also used to evaluate the effects of *FBN2* methylation with other explanatory variables on survival time, but the *FBN2* methylation was not a significant independent factor (data not shown).

4. Discussion

Tumor invasion is one of the earliest steps in the multistep process of metastasis and is characterized by cancer cells invading and breaking the basement membrane or other components of the extracellular matrix. Therefore, alteration of the extracellular matrix molecule is important for the development of malignant tumors [13]. *FBN2*, a large modular extracellular matrix glycoprotein found in many vertebrate organ systems, is known to be a key component of elastic fiber. Recently, Hagihara et al. demonstrated that *FBN2* is frequently methylated in pancreatic cancer [10]. However, there is no report on the role of *FBN2* in lung cancer. To understand the role of *FBN2* gene in lung cancer, we examined the expression of *FBN2*. It was expressed in tracheal cells, and cultured airway epithelial cells, whereas the lung cancer cell lines showed a loss of 50% of the expression. Treatment with 5-Aza-CdR restored the expression of the gene in RT-PCR-negative cell lines, indicating that methylation is a major mechanism of transcriptional silencing of the gene. Also, tumor-specific methylation of *FBN2* gene was present in 49% of NSCLC. Although other mechanisms for disruption of the extracellular matrix exist, such as inactivation of laminin5-encoding genes [14–16] or overexpression of matrix metalloproteinases [17,18], aberrant methylation of *FBN2* may be one of those participating in the process of tumor progression.

In our study, two cell lines showed a loss *FBN2* expression with a lack of aberrant methylation. This may have been due to other mechanisms of inactivating TSGs, such as loss of heterozygosity, point mutations, and homozygous deletions [19]. Also, we found *FBN2* methylation in some of the matched nonmalignant lung tissues. Possible explanations for detecting methylated alleles in the nonmalignant lung tissues are that they may represent premalignant changes [20], or be related to age [21] or smoking [22].

In this study, 49% of *FBN2* methylation was associated with an increase in tumor size, lymph node involvement, and advanced stages. Although further study will be required in order to understand the role of *FBN2* in the pathogenesis of advanced lung cancer, our data suggested that it is advantageous for tumor invasion and metastasis to downregulate *FBN2* gene of cancer cells. There are several reports about the correlation between the aberrant methylation of TSG and the progression of lung cancer [23,24]. *FBN2* may be added to the list of progression associated methylation genes of lung cancer because of the high frequency of methylation correlated significantly with progression. To

our knowledge, this is the first report that demonstrating the methylation of *FBN2* promoter in lung cancer and the correlation between *FBN2* methylation and lung cancer progression.

Our data did not show a significant association between *FBN2* methylation and patient survival. The lack of significance in the relationship of methylation to survival outcome may result from the limited number of patients taking part in our study, or on other factors.

In conclusion, we demonstrated frequent inactivation of *FBN2* gene through aberrant methylation of the promoter in NSCLC cell lines. We also found methylation of *FBN2* frequently in primary NSCLC; it correlated with the progression of the tumor from early to late stage disease. Aberrant methylation of *FBN2* gene appears to be an important factor in the pathogenesis of invasive NSCLC. Our findings of a frequent acquired tumor-related epigenetic alteration favor the candidacy of *FBN2* as a TSG.

Acknowledgements

This work was supported by a grant from Sasagawa Foundation Program. We thank Yusuke Suenaga, Biology Department, Faculty of Science, Chiba University, Japan for preparing cDNA. We greatly thank Dr. Toshikazu Ushijima, Chief, Carcinogenesis Division, National Cancer Center Research Institute, Japan for technical advice. We are also grateful to Mr. C.W. P. Reynolds for linguistic assistance with this manuscript.

References

- [1] Shigematsu H, Suzuki M, Takahashi T, Miyajima K, Toyooka S, Shivapurkar N, et al. Aberrant methylation of HIN-1 (high in normal-1) is a frequent event in many human malignancies. *Int J Cancer* 2005;113(4):600–4.
- [2] Sunaga N, Miyajima K, Suzuki M, Sato M, White MA, Ramirez RD, et al. Different roles for caveolin-1 in the development of non-small cell lung cancer versus small cell lung cancer. *Cancer Res* 2004;64(12):4277–85.
- [3] Marsit CJ, Liu M, Nelson HH, Posner M, Suzuki M, Kelsey KT. Inactivation of the Fanconi anemia/BRCA pathway in lung and oral cancers: implications for treatment and survival. *Oncogene* 2004;23(4):1000–4.
- [4] Gazdar AF, Miyajima K, Reddy J, Sathyanarayana UG, Shigematsu H, Suzuki M, et al. Molecular targets for cancer therapy and prevention. *Chest* 2004;125(5 Suppl.):975–1015.
- [5] Girard L, Zochbauer-Muller S, Virmani AK, Gazdar AF, Minna JD. Genome-wide allelotyping of lung cancer identifies new regions of allelic loss, differences between small cell lung cancer and non-small cell lung cancer, and loci clustering. *Cancer Res* 2000;60(17):4894–906.
- [6] Suzuki M, Sunaga N, Shames DS, Toyooka S, Gazdar AF, Minna JD. RNA interference-mediated knockdown of DNA methyltransferase 1 leads to promoter demethylation and gene re-expression in human lung and breast cancer cells. *Cancer Res* 2004;64(9):3137–43.
- [7] Toyooka S, Suzuki M, Tsuda T, Toyooka KO, Maruyama R, Tsukuda K, et al. Dose effect of smoking on aberrant methylation in non-small cell lung cancers. *Int J Cancer* 2004;110(3):462–4.
- [8] Toyooka S, Suzuki M, Maruyama R, Toyooka KO, Tsukuda K, Fukuyama Y, et al. The relationship between aberrant methylation and survival in non-small-cell lung cancers. *Br J Cancer* 2004;91(4):771–4.
- [9] Yang Q, Ota K, Tian Y, Kumar A, Wada J, Kashiwara N, et al. Cloning of rat fibrillin-2 cDNA and its role in branching morphogenesis of embryonic lung. *Dev Biol* 1999;212(1):229–42.
- [10] Hagihara A, Miyamoto K, Furuta J, Hiraoka N, Wakazono K, Seki S, et al. Identification of 27 5' CpG islands aberrantly methylated and 13 genes silenced in human pancreatic cancers. *Oncogene* 2004;23(53):8705–10.
- [11] Suzuki M, Shigematsu H, Takahashi T, Shivapurkar N, Sathyanarayana UG, Iizasa T, et al. Aberrant methylation of Reprimo in lung cancer. *Lung Cancer* 2005;47(3):309–14.
- [12] Suzuki M, Toyooka S, Miyajima K, Iizasa T, Fujisawa T, Bekele NB, et al. Alterations in the mitochondrial displacement loop in lung cancers. *Clin Cancer Res* 2003;9(15):5636–41.
- [13] Mücke P, Tman A. A: Tumour-stroma interaction: cancer-associated fibroblasts as novel targets in anti-cancer therapy? *Lung Cancer* 2004;45(Suppl. 2):S163–75.
- [14] Sathyanarayana UG, Maruyama R, Padar A, Suzuki M, Bondaruk J, Sagalowsky A, et al. Molecular detection of non-invasive and invasive bladder tumor tissues and exfoliated cells by aberrant promoter methylation of laminin-5 encoding genes. *Cancer Res* 2004;64(4):1425–30.
- [15] Sathyanarayana UG, Padar A, Huang CX, Suzuki M, Shigematsu H, Bekele BN, et al. Aberrant promoter methylation and silencing of laminin-5-encoding genes in breast carcinoma. *Clin Cancer Res* 2003;9(17):6389–94.
- [16] Sathyanarayana UG, Padar A, Suzuki M, Maruyama R, Shigematsu H, Hsieh JT, et al. Aberrant promoter methylation of laminin-5-encoding genes in prostate cancers and its relationship to clinicopathological features. *Clin Cancer Res* 2003;9(17):6395–400.
- [17] Iizasa T, Fujisawa T, Suzuki M, Motohashi S, Yasufuku K, Yasukawa T, et al. Elevated levels of circulating plasma matrix metalloproteinase 9 in non-small cell lung cancer patients. *Clin Cancer Res* 1999;5(1):149–53.
- [18] Suzuki M, Iizasa T, Fujisawa T, Baba M, Yamaguchi Y, Kimura H, et al. Expression of matrix metalloproteinases and tissue inhibitor of matrix metalloproteinases in non-small-cell lung cancer. *Invas Metast* 1998;18(3):134–41.
- [19] Shapiro GI, Park JE, Edwards CD, Mao L, Merlo A, Sidransky D, et al. Multiple mechanisms of p16INK4A inactivation in non-small cell lung cancer cell lines. *Cancer Res* 1995;55(24):6200–9.
- [20] Zochbauer-Muller S, Fong KM, Virmani AK, Geradts J, Gazdar AF, Minna JD. Aberrant promoter methylation of multiple genes in non-small cell lung cancers. *Cancer Res* 2001;61(1):249–55.
- [21] Ahuja N, Issa JP. Aging, methylation and cancer. *Histol Histopathol* 2000;15(3):835–42.
- [22] Vuilleminot BR, Pulling LC, Palmisano WA, Hutt JA, Belinsky SA. Carcinogen exposure differentially modulates RAR-beta promoter hypermethylation, an early and

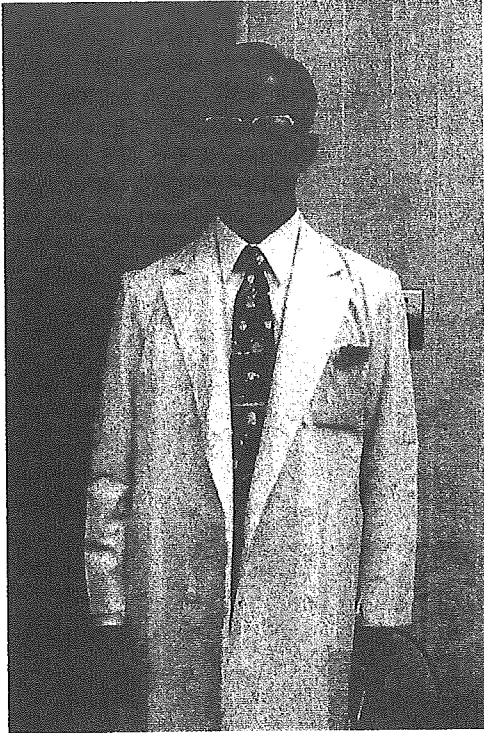
- frequent event in mouse lung carcinogenesis. *Carcinogenesis* 2004;25(4):623–9.
- [23] Kim DH, Nelson HH, Wiencke JK, Christiani DC, Wain JC, Mark EJ, et al. Promoter methylation of DAP-kinase: association with advanced stage in non-small cell lung cancer. *Oncogene* 2001;20(14):1765–70.
- [24] Seike M, Gemma A, Hosoya Y, Hemmi S, Taniguchi Y, Fukuda Y, et al. Increase in the frequency of p16INK4 gene inactivation by hypermethylation in lung cancer during the process of metastasis and its relation to the status of p53. *Clin Cancer Res* 2000;6(11):4307–13.

Available online at www.sciencedirect.com



OBITUARY

Professor Yoshiaki Tsuchida, MD, PhD (1936–2005)



Dr. Yoshiaki Tsuchida, a pediatric surgeon whose research focus was pediatric oncology, died on June 28th, 2005 at the age of 68 after a prolonged illness terminating in liver failure. At the end, he was surrounded by his loving wife, Mineko, and sons, Yasuaki and Naoaki.

Dr. Tsuchida was born on October 25th, 1936, in Osaka, Japan, and entered the University of Tokyo, Faculty of Medicine, in 1955 where he became an avid tennis player. After graduation in 1961, and a 1-year internship, he elected surgery for his future career and joined the Department of Surgery at the University of Tokyo. There, he met Prof. Masanobu Ishida, a pioneer in Japanese pediatric surgery, and he decided to make that his special field of concentration. After receiving his Ph.D. degree, he continued his investigations of the clinical import of alpha-fetoprotein (AFP) assays in pediatric solid tumors including teratomas and hepatoblastomas. This work resulted in his publication important quantitative data relevant to the normal serum levels of AFP in infants that decline rapidly after birth. This landmark work has been

frequently cited the literature and has been of great utility at the bedside.

Dr. Tsuchida was appointed Assistant in Surgery in 1967, an Instructor of Pediatric Surgery in 1969, and a Lecturer of Pediatric Surgery in 1975 in the University of Tokyo Hospital. He then moved to the National Children's Hospital in Tokyo in 1985 as the Head of the Department of Surgery. He returned to the University of Tokyo Hospital as Professor and Chairman of the Department of Pediatric Surgery in 1991. There, his research group established a series of transplantable neuroblastoma xenografts in nude mice, which were used to screen candidate clinical anti-cancer reagents. He was the leader of the nation-wide Japanese Neuroblastoma Study Group also for a long time, and was honored as its President to convene the 32nd Annual Meeting of the Japanese Society of Pediatric Surgeons in 1995.

One year before his expected retirement from the university, he was invited to become the Director of Gunma Children's Medical Center in Gunma prefecture, Japan. He continued his research work there, where his inspiring example stimulated young clinicians to undertake clinical research that can be termed "medical science at the bedside". For example, Dr. Hitoshi Ikeda, one of his trainees absorbed these teachings and published the first reports of the increasing incidence of hepatoblastoma in low-birth-weight babies. These observations, first made in Japan, have been confirmed both in U.S.A. and Europe.

Unlike many academic leaders in Japan, Dr. Tsuchida never worked in foreign countries. He encouraged his trainees, however, to gain experience abroad and bring back to Japan what they learned. Dr. Tsuchida saw this as a means of enriching Japanese pediatric oncology, a policy that has had ample rewards as the literature will attest.

Dr. Tsuchida himself wrote more than 220 papers in English, along with 151 other original articles and 16 book chapters. Amazingly, he presented 118 papers at international meetings where he was very active and exerted a profound world-wide influence. Together with Dr. Tadashi

Akira Nakagawara is the Chairman of Advances in Neuroblastoma Research, Chiba Cancer Center Research Institute.

*Correspondence to: Akira Nakagawara, Division of Biochemistry, Chiba Cancer Center Research Institute, 666-2 Nitona, Chuoh-ku, Chiba 260-8717, Japan. E-mail: akiranak@chiba-cc.jp

Received 19 July 2005; Accepted 19 July 2005